UAV-LEO Integrated Backbone: A Ubiquitous Data Collection Approach for B5G Internet of Remote Things Networks

Ting Ma, *Member, IEEE*, Haibo Zhou, *Senior Member, IEEE*, Bo Qian, *Student Member, IEEE*, Nan Cheng, *Member, IEEE*, Xuemin Shen, *Fellow, IEEE*, Xiang Chen, and Bo Bai, *Senior Member, IEEE*

***Abstract*— With the advance of unmanned aerial vehicles (UAVs) and low earth orbit (LEO) satellites, the integration of space, air and ground networks has become a potential solution to the beyond fifth generation (B5G) Internet of remote things (IoRT) networks. However, due to the network heterogeneity and the high mobility of UAVs and LEOs, how to design an efficient UAV-LEO integrated data collection scheme without infrastructure support is very challenging. In this paper, we investigate the resource allocation problem for a two-hop uplink UAV-LEO integrated data collection for the B5G IoRT networks, where numerous UAVs gather data from IoT devices and transmit the IoT data to LEO satellites. In order to maximize the data gathering efficiency in the IoT-UAV data gathering process, we study the bandwidth allocation of IoT devices and the 3-dimensional (3D) trajectory design of UAVs. In the UAV-LEO data transmission process, we jointly optimize the transmit powers of UAVs and the selections of LEO satellites for the total uploaded data amount and the energy consumption of UAVs. Considering the relay role and the cache capacity limitations of UAVs, we merge the optimizations of IoT-UAV data gathering and UAV-LEO data transmission into an integrated optimization problem, which is solved with the aid of the successive convex approximation (SCA) and the block coordinate descent (BCD) techniques. Simulation results demonstrate that the proposed scheme achieves better performance than the benchmark algorithms in terms of both energy consumption and total upload data amount.**

***Index Terms*— B5G IoRT, UAV-LEO integrated data collection, resource allocation, 3D trajectory design.**

Manuscript received October 16, 2020; revised February 22, 2021; accepted April 12, 2021. Date of publication June 14, 2021; date of current version October 18, 2021. This work was supported in part by the National Key Research and Development Program of China under Grant 2020YFB1806104, in part by the Natural Science Foundation Jiangsu Province Youth Project under Grant BK20180329, in part by the Innovation and Entrepreneurship of Jiangsu Province High-Level Talent Program, in part by the Summit of the Six Top Talents Program Jiangsu Province, and in part by the Natural Sciences and Engineering Research Council of Canada (NSERC). *(Corresponding author: Haibo Zhou.)*

Ting Ma, Haibo Zhou, and Bo Qian are with the School of Electronic Science and Engineering, Nanjing University, Nanjing 210023, China (e-mail: majiawan27@163.com; haibozhou@nju.edu.cn; boqian@smail.nju.edu.cn).

Nan Cheng is with the School of Telecommunication Engineering and the State Key Laboratory of ISN, Xidian University, Xi'an 710071, China (e-mail: dr.nan.cheng@ieee.org).

Xuemin Shen is with the Department of Electrical and Computer Engineering, University of Waterloo, Waterloo, ON N2L 3G1, Canada (e-mail: sshen@uwaterloo.ca).

Xiang Chen and Bo Bai are with the Theory Lab, 2012 Labs, Huawei Technologies Co., Ltd., Hong Kong (e-mail: chenxiang73@huawei.com; ee.bobbai@gmail.com).

Color versions of one or more figures in this article are available at https://doi.org/10.1109/JSAC.2021.3088626.

Digital Object Identifier 10.1109/JSAC.2021.3088626

I. Introduction

With the increasing demands of seamless and ubiquitous network access in the beyond fifth generation (B5G), the integration of space, air, and ground (SAG) networks has attracted rising attention, which significantly benefits the B5G Internet of remote things (IoRT) [1]–[4]. The IoRT network has been widely adopted in various applications, for instance, the remote surveillance systems for monitoring wild animals, natural disasters and climate change [5]–[7]. However, in remote areas, the ground base station (GBS) is usually difficult to deploy due to geographical limitation or high cost, which leads to that the data cached in distributed IoT devices have to be forwarded to a far data center for further analysis. Hence, reliable and efficient data collection and data transmission in IoRT networks are of great significance.

The satellite communication system can offer seamless wireless access to wide geographical areas, and provide an efficient solution to the IoRT where GBSs are usually not available [5], [8]. Comparing to traditional satellite systems of medium earth orbit (MEO) and geostationary earth orbit (GEO), the low earth orbit (LEO) satellite has the advantages of small propagation loss, low propagation delay and global coverage [9]. However, there are also many challenges in the LEO satellites assisted IoRT networks. Considering the huge number of IoT devices in the ground and the long transmission delay for the data transmission, it is usually not feasible to directly access numerous IoT devices to the satellite constellation [10]. Meanwhile, the IoT device is difficult to achieve long-distance transmission due to its transmit power and energy consumption limitations.

Recently, the significant development of unmanned aerial vehicles (UAVs) has been witnessed. According to the report [11], the global market for UAV estimated at $24.3 billion in 2020 is expected to reach $77.5 billion by 2027, growing at a compound annual growth rate of 18% over the analysis period 2020-2027. Moreover, the UAV-based networks have attracted much interest and investigations in various applications [12]–[15]. Considering the benefits of high mobility, economic and flexible deployment, and line-of-sight (LoS) transmission [16], [17], the UAV swarm can be efficiently applied to the B5G IoRT networks as a relay for data transmission. The UAV swarm can assist LEO satellites to improve the SAG channel capacity, achieve seamless cov-

erage, and dynamically move to IoT devices and transmit the collected data to LEO satellites. However, when introducing the UAV as a relay in the B5G IoRT networks, the uplink data collection becomes more challenging because of the different channel characteristics of UAV-ground and UAV-satellite links, high mobility of UAVs and LEO satellites, cache capacity limitations of UAVs, etc.

In this paper, for the hierarchical UAV-LEO integrated data collection in the B5G IoRT networks assisted with UAV swarm relays, we divide the two-hop uplink communication task into two layers, i.e., IoT-UAV data gathering as layer 1, and UAV-LEO data transmission as layer 2. For layer 1, we first divide the IoT devices into different areas based on their geographic locations due to the wide range of surveillance, and one UAV gathers data from IoT devices in each area. To achieve the high transmission rate of each IoT device during the mission time period in each area, we maximize the average achievable rate of each IoT device by optimizing the uplink bandwidth allocation of IoT devices and the 3D trajectory of the UAV. For layer 2, in order to maximize the uploaded data amount from UAVs to LEO satellite constellation and minimize the energy consumption of UAVs, we optimize the transmit powers of UAVs and the selections of LEO satellites. Meanwhile, considering the limited cache capacity of UAV relays, we merge optimizations of layer 1 and layer 2 into an integrated optimization problem and propose a block coordinate descent (BCD) based framework to solve it.

The main contributions of the paper are summarized as follows:

- *Hierarchical SAG-IoRT network design:* We propose a UAV swarm and LEO satellite constellation assisted data collection for the B5G IoRT networks. The task consists of the IoT-UAV data gathering and UAV-LEO data transmission, which can achieve reliable and efficient IoRT data collection without infrastructure support.
- *IoT bandwidth allocation and UAV 3D trajectory design:* To optimize the data gathering efficiency of UAVs, we propose the bandwidth allocation of IoT devices and the 3D trajectory of UAVs by leveraging successive convex approximation (SCA) and BCD techniques.
- *UAV power allocation and LEO satellite selection:* To optimize the data transmission process from UAVs to LEO satellites, we optimize the transmit powers of UAVs and the selections of LEO satellite constellation by using the Lagrangian dual decomposition method.
- *Joint optimization and computational complexity analysis:* We propose a BCD-based approach to solve the above two layer optimizations alternately. Meanwhile, we analyze the computational complexity and its convergence towards at least a locally optimal solution for the BCD based approach.

The remainder of the paper is organized as follows. Section II reviews the related works. The system model and problem formulation are described in Section III. Section IV provides the problem solution. Section V presents the simulation results, and Section VI concludes the paper.

II. Related Works

In the literature, several works have been appeared for the UAV-assisted ground devices data collection. In [18], Wang *et al.* proposed a UAV-assisted IoT network, where the UAV is deployed as an anchor node and aerial data collector, and assists the base station (BS) for device positioning and data collecting. In [19], Sun *et al.* studied the optimal 3D trajectory design and resource allocation for maximization of the system sum throughput over a given time period in the UAV communication systems. In [20], Mozaffari *et al.* analyzed the deployment of UAVs as BSs for the ground user (GU) communication, while the trade-off between delay and coverage is also argued. In [21], Zhang *et al.* considered a UAV-enabled radio access network where the UAV serves as the aerial platform to communicate with GUs, and proposed iterative algorithms to perform joint UAV trajectory and communication resource allocation optimization such that the UAV periodic flight duration is minimized. In [22], Wu *et al.* investigated a multi-UAV enabled wireless communication system with multiple UAVs employed as aerial BSs to serve GUs. To achieve fair performance over all GUs, the minimum throughput in the downlink communication is maximized via joint trajectory and communication design. In [23], taking the energy consumption of UAVs into account, Cai *et al.* studied the trajectory and resource allocation design for downlink energy-efficient secure UAV communication systems. However, due to the communication distance and power energy limitations of UAVs, the UAV-assisted communication is difficult to ensure that data in IoRT networks are transmitted to the far data center in a timely manner.

To address these issues, satellites are considered in the B5G IoRT networks. In [24], Li *et al.* introduced the coordination of UAVs with hybrid GEO satellite-terrestrial networks to enhance the maritime coverage. Under some limitations such as backhaul and energy capacity and UAV kinematics, they jointly optimized the UAV trajectory and transmit power. In [25], Wang *et al.* applied the Lagrangian dual decomposition method to solve a two-stage joint hovering altitude design and power control for the SAG IoT networks. Jia *et al.* [9] minimized the total energy consumption of UAVs for the LEO satellite assisted UAV data collection in the IoRT while satisfying the IoRT demands. In [26], Wang *et al.* considered a SAG-IoRT framework, and proposed an iterative algorithm to optimize the system capacity via jointly designing power control, smart devices connection scheduling and UAV's trajectory. Most of the existing works are concentrated on a single LEO satellite scenario, where the focus is on the optimization of IoT devices to UAVs. However, in practice, a surveillance area is often covered by multiple LEO satellites due to the wide coverage of satellites. Therefore, in this paper, we will consider the optimization on not only the bandwidth allocation of IoT devices and the 3D trajectory design of UAVs, but also the power control of UAVs and access selections to LEO satellites. To the best of our knowledge, this is the first work to consider these performance indicators simultaneously for the SAG-IoRT networks.

Notations: The scalars and matrices are written as italic letters and bold-face lower-case letters, respectively. Let $\mathbb{R}^n$

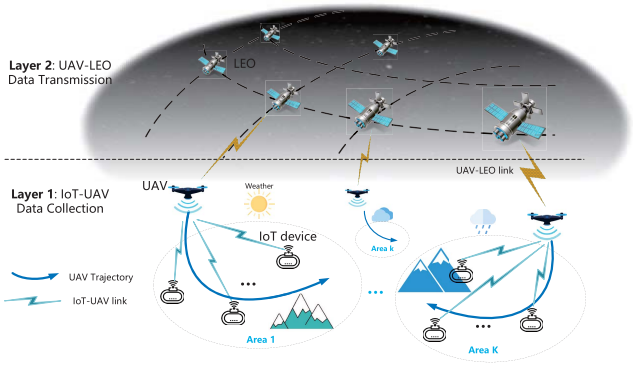

Fig. 1. The UAV-LEO integrated data collection scenario in the B5G IoRT networks.

be the space of n-dimensional real vectors, and $\mathbf{I}$ represent the identity matrix with proper dimension. For a matrix $\mathbf{X} \in \mathbb{R}^{n\times m}$, define its Frobenius norm as $\|\mathbf{X}\|$ (the Euclidean norm of a vector is its special case). Denote $\log_2(\cdot)$ as the logarithm with base 2. Denote $\dot{\mathbf{q}}(n)$ as the first-order derivative of a time-varying function $\mathbf{q}(n)$ with respect to time slot n. For a continuously differentiable function $f(x)$, let $\nabla f(x)$ and $\nabla^2 f(x)$ be the first and second order derivatives of $f(x)$, respectively.

III. System Modeling

As shown in Fig. 1, we investigate the UAV-LEO integrated data collection scheme in the B5G IoRT networks, where massive IoT devices get data and then transmit these data to a far ground data center through uplinks by leveraging on UAV swarms and LEO satellites. Assume that there are overall M IoT devices distributed in K disjoint areas with Area k having N_k IoT devices, i.e., $\sum_{k=1}^{K} N_k = M$. Denote $\mathcal{I}_k = \{I_{1,k}, \ldots, I_{N_k,k}\}$ as the set of IoT devices in Area k, $k = 1, \ldots, K$. In our setup, one UAV is designated to gather data of IoT devices within each area. Hence, K UAVs are deployed in the air. Let $\mathcal{U} = \{U_1, \ldots, U_K\}$ be the set of UAVs with UAV U_k soaring in Area k, $k = 1, \ldots, K$. In our setup, we consider the ultra-dense LEO satellite constellation (tens of thousands of LEO satellites), and there are always multiple LEO satellites serving these K UAVs during a short time. Each UAV chooses the proper LEO satellite to handover its data, and these LEO satellites can temporally store their received data and transmit them to the data center on the ground eventually. In this paper, we only consider data collection through uplinks.

During an appointed mission period of T, we aim to design an optimal UAV and LEO satellite assisted scheduling mechanism for data collection from the B5G IoRT networks, which maximizes the total received data amount of LEO satellites from IoT devices and minimizes the total energy consumption of UAVs without data backlogs at UAVs. For the convenience of follow-up analyses, we divide the mission time period T equally into N time slots with a slot length δ, i.e., $T = N\delta$. Denote $\mathcal{N} = \{1, 2, \ldots, N\}$ to represent the time slot set. At time slot n, we assume that there are L_n LEO satellites serving these K UAVs in the region, and the serving relationship between LEO satellites and UAVs are unchanged.

TABLE I
Main Notations

Notation	Meaning
K	Number of areas
M, N_k	Numbers of all IoT devices and IoT devices in Area k
L	Number of LEO satellites
N	Number of time slots
δ	Time slot length
$I_{i,k}$	The i-th IoT device in Area k
U_k	The UAV in Area k
$\mathbf{s}_{i,k}$	Position of IoT device $I_{i,k}$
$\mathbf{q}_{k,n}$	Position of UAV U_k at time slot n
$d_{\min}$	Minimum safe distance between UAVs and IoT devices
ρ_0	Channel power gain at the reference distance of $d_0 = 1$ m
$h_{i,k,n}$	Channel power gain between IoT device $I_{i,k}$ and UAV U_k
$a_{i,k,n}$	Fraction of the total bandwidth in Area k that is allocated for IoT device $I_{i,k}$ at time slot n
B	Total available bandwidth for each UAV
$p_{i,k}$	Transmit power of $I_{i,k}$
N_0	Additive white Gaussian noise power spectral density
$r_{i,k,n}$	Instantaneous achievable rate
$b_{k,l,n}$	Uplink transmission indicator variable from UAV k to LEO satellite l at time slot n
$\nu(c)$	Fading coefficient with the channel condition c
$g(p,c)$	Transmission rate function for power p and channel state c
$c_{k,l,n}$	Channel state of uplink between UAV k and LEO satellite l at time slot n
$P_{k,l,n}$	Power allocated on the uplink between UAV k and LEO satellite l at time slot n
W	Bandwidth of each uplink channel from UAV to LEO
$D_k^u(N')$	Overall uploaded data amount of UAV k till time slot N'
$D_k^r(N')$	Overall received data amount of UAV k till time slot N'
C_k	Cache capacity of UAV k
E_k	Total energy consumption of UAV k
$V_{\max}$	Maximum speed of UAV

Important notations are listed in Table I.

A. IoT-UAV Data Gathering

These K areas are supposed to be far away from each other. That is to say, there is no interference among different areas, and data gathering of each area is independent. Hence, we take Area k as an example to analyze the data gathering of UAV U_k from IoT devices $\mathcal{I}_k$.

Since IoT devices may be deployed in mountain regions, we assume the coordinate of IoT device $I_{i,k}$ is $\mathbf{s}_{i,k} \in \mathbb{R}^3$ and the time-varying coordinate of UAV U_k is $\mathbf{q}_{k,n} \in \mathbb{R}^3$ at time slot n. The uplinks from IoT devices to UAV U_k are dominated by LoS. Hence, the channel gain $\tilde{h}_{i,k,n}$ between IoT device $I_{i,k}$ and UAV U_k at time slot n is

$$\tilde{h}_{i,k,n} = \rho_0 d_{i,k,n}^{-2} = \frac{\rho_0}{\|\mathbf{q}_{k,n} - \mathbf{s}_{i,k}\|^2},$$

where ρ_0 is the channel power gain at the reference distance of $d_0 = 1$ m and $d_{i,k,n}$ is the distance between $I_{i,k}$ and U_k at time slot n. Remarkably, UAVs cannot fly too close to IoT devices due to collision avoidance. Hence, we modify the channel gain of IoT device $I_{i,k}$ as follows:

$$h_{i,k,n} = \frac{\rho_0}{\max(\|\mathbf{q}_{k,n} - \mathbf{s}_{i,k}\|^2, d_{\min}^2)}, \tag{1}$$

where $d_{\min}$ is the minimum safe distance between UAV and IoT devices for collision avoidance.

Suppose that the UAV adopts frequency division multiple access (FDMA) with dynamic bandwidth allocation among all IoT devices, that is, the UAV can receive data from multiple IoT devices at one time slot. Denote $a_{i,k,n}$ as the bandwidth fraction that is allocated for $I_{i,k}$ at time slot n. Then, variable $a_{i,k,n}$ should satisfy:

$$\sum_{i=1}^{N_k} a_{i,k,n} \leqslant 1, \quad \forall\ k, n,$$
$$a_{i,k,n} \geqslant 0, \quad \forall\ i, k, n.$$

This scheme includes time division multiple access (TDMA) with dynamic time scheduling ($a_{i,k,n}$ is a binary variable) and FDMA with fixed bandwidth allocation ($a_{i,k,n} = a_{i,k},\ \forall n$) as special cases.

Denote the total available bandwidth of each UAV by B, and assume that IoT device $I_{i,k}$ uploads its sensing data with a prescribed transmit power $p_{i,k}$, $i = 1, \ldots, N_k$. Subsequently, when IoT device $I_{i,k}$ transmits data to the UAV (i.e., $a_{i,k,n} > 0$), the instantaneous achievable rate in bits/second (bits/s) for IoT device $I_{i,k}$ is presented as

$$\begin{aligned} r_{i,k,n} &= a_{i,k,n} B \log_2\left(1 + \frac{p_{i,k} h_{i,k,n}}{a_{i,k,n} B N_0}\right) \\ &= a_{i,k,n} B \\ &\times \log_2\left(1 + \frac{p_{i,k}\rho_0}{\max(\|\mathbf{q}_k(n) - \mathbf{s}_{ki}\|^2, d_{\min}^2) a_{i,k,n} B N_0}\right), \end{aligned} \quad (2)$$

where $p_{i,k}$ stands for the transmit power of $I_{i,k}$, B is the total available bandwidth of Area k, and N_0 represents the additive white Gaussian noise (AWGN) power spectral density.

Then, the average achievable rate of IoT device $I_{i,k}$ during all time slots is formulated as

$$\frac{1}{N} \sum_{n \in \mathcal{N}} r_{i,k,n}.$$

In each area, via optimizing the UAV's trajectory and bandwidth allocation, we can maximize the minimum average achievable rate over all IoT devices in this area.

B. UAV-LEO Data Transmission

For data uplink transmission between UAVs and LEO satellites, let $b_{k,l,n}$ be the 0-1 binary indicator variable of time-varying uplink between UAV k and LEO satellite l at time slot n, $k \in \mathcal{K} = \{1, \ldots, K\}$, $l \in \mathcal{L}_n = \{1, \ldots, L_n\}$, $n \in \mathcal{N}$. When there exists an uplink transmission from UAV k to LEO satellite l at n, we let $b_{k,l,n} = 1$, and otherwise $b_{k,l,n} = 0$. We assume that one UAV transmits data to at most one LEO satellite at one time slot. Hence, it holds

$$\sum_{l \in \mathcal{L}_n} b_{k,l,n} \leqslant 1, \quad \forall k,\ n,$$
$$b_{k,l,n} = \{0, 1\}, \quad \forall k,\ l,\ n.$$

Similar to [27], to avoid data upload overlapping, we divide the frequency bandwidth for UAV satellite uplinks into a group of orthogonal subchannels by exploiting the Orthogonal Frequency Division Multiplexing (OFDM) technology. Then we assume that different UAVs utilize different orthogonal subchannels to connect to the same LEO at the same time slot. That is to say, there is no interference at the LEO satellites. As in [27], we present the relationship between transmission rate and power allocation of an uplink referring to the concave rate-power curve. According to [27], for given channel condition c, transmit power p and bandwidth W, the classic Shannon's Theorem based rate-power function $g(p, c)$ in bits/s is obtained as

$$g(p, c) = W \log_2(1 + \nu(c) \cdot p), \quad (3)$$

where $\nu(c)$ represents the fading coefficient under c. We also use the three-state condition model [28], where $\nu(c)$ equals 1.0, 3.46 and 5.03, which corresponds to the bad, medium and good conditions based on weather conditions. Obviously, $g(p, c)$ is a concave function of p.

Define $c_{k,l,n}$ as the time-varying channel state of uplink between UAV k and LEO satellite l at n. We can get $c_{k,l,n}$ from either direct measurement by some communication systems [29] or prediction based on existing channel states by a linear prediction equation [28]. Then, $c_{k,l,n}$ can be assumed to be known by the system controller all the time in our framework. Additionally, we denote variable $P_{k,l,n}$ as the power allocated to the uplink between UAV k and LEO satellite l at n. Then the total uploaded data amount of UAV k to LEO satellites during N time slots is

$$D_k^{tu} = \sum_{n \in \mathcal{N}} \sum_{l \in \mathcal{L}_n} b_{k,l,n} \cdot g(P_{k,l,n}, c_{k,l,n}) \cdot \delta. \quad (4)$$

To avoid data backlogs in UAVs at arbitrary time slot, the uplink transmission data amount of UAV k should be smaller than its received data amount from IoT devices in a prescribed threshold. Specifically, till arbitrary time slot $N' \in \mathcal{N}$, the overall uploaded data amount of UAV k can be calculated as

$$D_k^u(N') = \sum_{n \leqslant N'} \sum_{l \in \mathcal{L}_n} b_{k,l,n} \cdot g(P_{k,l,n}, c_{k,l,n}) \cdot \delta. \quad (5)$$

According to arguments in Subsection III-A, the overall received data amount of UAV k from IoT devices till N' is formulated as

$$D_k^r(N') = \sum_{n \leqslant N'} \sum_{i=1}^{N_k} r_{i,k,n} \cdot \delta. \quad (6)$$

As a consequence, denoting the cache capacity of UAV k as C_k, the following relationship should hold true:

$$D_k^r(N') - D_k^u(N') \leqslant C_k, \quad \forall k,\ \forall N'. \quad (7)$$

Meanwhile, the power supply of UAVs is the bottleneck resource. Hence, when a UAV uploads data to LEO satellites, we should minimize its energy consumption. The total energy consumption of UAV k spent on data-uploading during time period T can be calculated as

$$E_k = \sum_{n \in \mathcal{N}} \sum_{l \in \mathcal{L}_n} b_{k,l,n} \cdot P_{k,l,n} \cdot \delta. \quad (8)$$

To optimize the total uploaded data amount to LEO satellites and the energy consumption simultaneously, we introduce a penalty function which positively associates with the total uploaded data amount D_k^{tu} in Eq. (4) and reversely associates with the energy consumption E_k in Eq. (8). Then, the penalty function can be denoted by

$$F_k := D_k^{tu} - \beta E_k, \tag{9}$$

where β is the weight of energy consumption.

By maximizing the penalty function F_k with respect to $b_{k,l,n}$ and $P_{k,l,n}$, we can get the optimal data transmitting mechanism from UAVs to LEO satellites. Remarkably, the involved term D_k^r in (7) is relevant to the instantaneous achievable rate $r_{i,k,n}$ in Eq. (2), which depends on the trajectory and bandwidth allocation of UAV k. Hence, the optimization of transmission from UAVs to LEO satellites is related to the transmission from IoT devices to UAVs.

C. Integrated Optimization on Uplink Data Collection

Based on the arguments in Subsections III-A and III-B, we can present the integrated optimization problem (IOP) as that LEO satellites collect data from IoT devices with UAV relaying. Denote $\mathcal{Q}_k = \{\mathbf{q}_{k,n}\}$ as the trajectory of UAV k, $\mathcal{A}_k = \{a_{i,k,n}\}$ represents the bandwidth allocation among IoT devices in Area k, and let $\mathcal{B} = \{b_{k,l,n}\}$ and $\mathcal{P} = \{P_{k,l,n}\}$ be the indicator variable set and the power allocation of UAVs, respectively. Then, IOP can be expressed as

$$\begin{aligned}
\text{IOP}: \quad & \max_{\substack{\eta_k, \mathcal{A}_k, \mathcal{Q}_k, \\ \mathcal{B}, \mathcal{P}}} \quad \sum_{k\in\mathcal{K}} \eta_k + F_k \\
& \text{s.t.} \ \frac{1}{N}\sum_{n\in\mathcal{N}} r_{i,k,n} \geqslant \eta_k, \quad \forall i,k, && \text{(c1)} \\
& \mathbf{q}_{k,0} = \mathbf{q}_{k,N}, \quad \forall k, && \text{(c2)} \\
& \|\dot{\mathbf{q}}_{k,n}\| \leqslant V_{\max}, \quad \forall k,n, && \text{(c3)} \\
& \sum_{i=1}^{N_k} a_{i,k,n} \leqslant 1, \quad \forall k,n, && \text{(c4)} \\
& a_{i,k,n} \geqslant 0, \quad \forall i,k,n, && \text{(c5)} \\
& P_{k,l,n} \geqslant 0, \quad \forall k,l,n, && \text{(c6)} \\
& P_{k,l,n} \leqslant P_{\max}, \quad \forall k,l,n, && \text{(c7)} \\
& D_k^r(N') \geqslant D_k^u(N'), \quad \forall k, N' \in \mathcal{N}, && \text{(c8)} \\
& D_k^r(N') - D_k^u(N') \leqslant C_k, \ \forall k,n, && \text{(c9)} \\
& \sum_{k\in\mathcal{K}} b_{k,l,n} g(P_{k,l,n}, c_{k,l,n}) \leqslant R_{\max}, \quad \forall l,n, && \text{(c10)} \\
& \sum_{l\in\mathcal{L}_n} b_{k,l,n} \leqslant 1, \quad \forall k,n, && \text{(c11)} \\
& b_{k,l,n} \in \{0,1\}, \quad \forall k,l,n. && \text{(c12)}
\end{aligned}$$

Constraint (c1) together with the term "$\max\ \eta_k$" in the objective function means maximizing the minimum average achievable rate among all IoT devices in each area. Constraint (c2) gives the constraint on UAVs' initial and final locations, which is meaningful in practical scenarios such as periodical data collections [21], and constraint (c3) is the velocity limit of UAVs. Constraints (c4) and (c5) are limitations of bandwidth allocation. Constraints (c6) and (c7) are the minimum and the maximum transmit power constraints on UAVs, respectively. Constraint (c8) is a natural constraint that the overall upload data amount of each UAV should not exceed its received data amount from IoT devices, while constraint (c9) avoids data backlogs in UAVs. Constraint (c10) implies the total data uploading rate of each LEO satellite cannot exceed the maximum data receiving rate $R_{\max}$, and constraints (c11) and (c12) are limitations on the choice of LEO satellites. By solving IOP, during the allocated mission time period T, we can maximize the minimum average achievable rate among all IoT devices as well as the data amount that IoT devices transmit to LEO satellites, and minimize the energy consumption of UAVs without data backlogs in UAVs.

For the proposed IOP, variables $\{\mathcal{A}_k, \mathcal{Q}_k, \mathcal{B}, \mathcal{P}\}$ are all or partly coupled in the objective function as well as constraints (c1), (c8)-(c10), which leads to their non-convexities. Moreover, the 0-1 constraint (c12) is also non-convex. Therefore, IOP is difficult to handle. To obtain the solution to this problem, a widely used method is the well-known BCD technique [21], [30]–[33]. That is, dividing IOP into two subproblems, and then repeatedly and alternatively solve these two subproblems until the objective function value changes within a prescribed threshold. Specifically, we divide IOP into bandwidth allocation and trajectory $(\mathcal{A}_k, \mathcal{Q}_k)$ optimization with fixed $(\mathcal{B}, \mathcal{P})$ in IoT-UAV data gathering, and power allocation and uplink selection $(\mathcal{B}, \mathcal{P})$ optimization with fixed $(\mathcal{A}_k, \mathcal{Q}_k)$ in UAV-LEO data transmission.

IV. Problem Solution

In this section, IOP is divided into two sub-problems: bandwidth allocation and trajectory optimization, and power allocation and uplink selection optimization. We argue how to solve the two sub-problems separately, and then use the BCD technique to get the solution to IOP.

A. Sub-Problem 1: Bandwidth Allocation and Trajectory Optimization With Fixed Power Allocation and Uplink Selection

For fixed power allocation and uplink selection $(\mathcal{B}, \mathcal{P})$, we design the optimal trajectory for each UAV by solving IOP. Considering that each UAV's trajectory is independent of others', we design the optimal trajectory of the UAV in Area k as an example, and we omit the index k for notation brevity. For this area, removing irrelevant terms with $\mathcal{A} = \{a_{i,n}\}$ and $\mathcal{Q} = \{\mathbf{q}_n\}$, IOP is transformed to

$$\begin{aligned}
(\text{SP1}) \quad & \max_{\eta, \mathcal{A}, \mathcal{Q}} \quad \eta \\
& \text{s.t.} \ \frac{1}{N}\sum_{n\in\mathcal{N}} r_{i,n} \geqslant \eta, \quad \forall i, && \text{(10a)} \\
& \mathbf{q}_0 = \mathbf{q}_N, && \text{(10b)} \\
& \|\mathbf{q}_{n+1} - \mathbf{q}_n\|^2 \leqslant \delta^2 V_{\max}^2, \ \forall n, && \text{(10c)} \\
& \sum_{i=1}^{N_k} a_{i,n} \leqslant 1, \ \forall\ n, && \text{(10d)}
\end{aligned}$$

$$a_{i,n} \geqslant 0,\ \forall\ i,n, \tag{10e}$$
$$D^r(N') \geqslant D^u(N'),\ \forall N' \in \mathcal{N}, \tag{10f}$$
$$D^r(N') \leqslant D^u(N') + C,\ \forall N' \in \mathcal{N}, \tag{10g}$$

where constraint (10c) is an equivalence of constraint (c3) in IOP, while expressions of $r_{i,n}$ and $D^r(N')$ are

$$r_{i,n} = a_{i,n} B \log_2 \left(1 + \frac{p_i \rho_0}{\max(\|\mathbf{q}_n - \mathbf{s}_i\|^2, d_{\min}^2) a_{i,n} B N_0}\right)$$

and

$$D^r(N') = \sum_{n \leqslant N'} \sum_{i=1}^{N_k} r_{i,n} \cdot \delta,$$

respectively. For fixed $(\mathcal{B}, \mathcal{P})$, $D^u(N')$ is a known constant for arbitrary N'. Since variables $\mathcal{A}$ and $\mathcal{Q}$ are coupled in $r_{i,n}$, similar to [21], [30], we again use the BCD approach to solve problem (SP1).

1) Bandwidth Allocation Optimization With Fixed Trajectory: Supposing that the trajectory $\mathcal{Q} = \{\mathbf{q}_n\}$ is fixed, then problem (SP1) is evolved to

$$\begin{aligned}
(\text{SP1-1})\ \max_{\eta, \mathcal{A}}\ & \eta \\
\text{s.t. } & \frac{1}{N} \sum_{n \in \mathcal{N}} r_{i,n} \geqslant \eta, \quad \forall i, && \text{(11a)} \\
& \sum_{i=1}^{N_k} a_{i,n} \leqslant 1,\ \forall\ n, && \text{(11b)} \\
& a_{i,n} \geqslant 0, \quad \forall\ i,n, && \text{(11c)} \\
& \sum_{n \leqslant N'} \sum_{i=1}^{N_k} r_{i,n} \delta \geqslant D^u(N'), \quad \forall N', && \text{(11d)} \\
& \sum_{n \leqslant N'} \sum_{i=1}^{N_k} r_{i,n} \delta \leqslant D^u(N') + C, \quad \forall N'. && \text{(11e)}
\end{aligned}$$

Denoting $\Delta_1 = \frac{p_i \rho_0}{\max(\|\mathbf{q}_n - \mathbf{s}_i\|^2, d_{\min}^2) B N_0}$ for notation brevity, let $r_{i,n} = r_1(a_{i,n}) = a_{i,n} B \log_2 \left(1 + \frac{\Delta_1}{a_{i,n}}\right)$. Due to

$$\nabla^2 r_1(a) = \frac{B \Delta_1}{(a + \Delta_1) \ln 2} \left(\frac{1}{a + \Delta_1} - \frac{1}{a}\right) < 0,$$

we conclude that $r_1(a_{i,n})$ is a concave function of $a_{i,n}$. Hence, except for constraint (11e), all other constraints are convex. To cope with the non-convexity of (11e), we use the SCA technique to relax it.

For the clarity and integrity, before relaxing constraint (11e), we first present the following well-known result.

Lemma 1: (Proposition B.3 in [34]) For a convex function $f(x)$, it can be lower bounded by

$$f(x) \geq f(x_0) + \nabla f(x_0)(x - x_0),$$

where x_0 is a given point in the domain of f. Moreover, $f(x) = f(x_0)$ if and only if $x = x_0$.

Since $r_1(a_{i,n})$ is concave with respect to $a_{i,n}$, according to Lemma 1, we can relax $r_{i,n} = r_1(a_{i,n})$ by its upper bound

$$\begin{aligned}
\hat{r}(a_{i,n}) &= r_1(a_{i,n}^t) + \nabla r_1(a_{i,n}^t)(a_{i,n} - a_{i,n}^t) \\
&= \frac{B \Delta_1 (a_{i,n}^t - a_{i,n})}{(a_{i,n}^t + \Delta_1) \ln 2} + a_{i,n} B \log_2 \left(1 + \frac{\Delta_1}{a_{i,n}^t}\right),
\end{aligned}$$

where $a_{i,n}^t$ is given. Obviously, we have $r(a_{i,n}) \leqslant \hat{r}(a_{i,n})$ and $\hat{r}(a_{i,n})$ is convex with respect to $a_{i,n}$. Consequently, we relax problem (SP1-1) to

$$\begin{aligned}
(\text{SP1-2})\ \max_{\eta, \mathcal{A}}\ & \eta \\
\text{s.t. } & \text{(11a), (11b), (11c), (11d)} \\
& \sum_{n \leqslant N'} \sum_{i=1}^{N_k} \hat{r}(a_{i,n}) \delta \leqslant D^u(N') + C, \quad \forall N', && \text{(12)}
\end{aligned}$$

where we replace constraint (11e) in problem (SP1-1) by the convex constraint (12). Therefore, problem (SP1-2) is a convex programming that can be solved efficiently by CVX [35].

Constraint (12) is more conservative than the original constraint (11e). Hence, the optimal solution of problem (SP1-2) is a lower bound of that of problem (SP1-1). To improve the quality of the solution, we iteratively solve problem (SP1-2) multiple times. According to [36], with a feasible initial point, the iterative procedure is convergent to a saddle point or a local minimum. As a consequence, with fixed trajectory, we can get the optimal bandwidth allocation.

2) Trajectory Optimization With Fixed Bandwidth Allocation: For fixed bandwidth allocation, by removing irrelevant terms with $\mathcal{A}$, we reduce problem (SP1) to

$$\begin{aligned}
(\text{SP1-3})\ \max_{\eta, \mathcal{Q}}\ & \eta \\
\text{s.t. } & \frac{1}{N} \sum_{n \in \mathcal{N}} r_{i,n} \geqslant \eta, \quad \forall i, && \text{(13a)} \\
& \mathbf{q}_0 = \mathbf{q}_N, && \text{(13b)} \\
& \|\mathbf{q}_{n+1} - \mathbf{q}_n\|^2 \leqslant \delta^2 V_{\max}^2, \quad \forall n, && \text{(13c)} \\
& D^r(N') \geqslant D^u(N'), \quad \forall N' \in \mathcal{N}, && \text{(13d)} \\
& D^r(N') \leqslant D^u(N') + C, \quad \forall N' \in \mathcal{N}, && \text{(13e)}
\end{aligned}$$

Note that, $r_{i,n}$ is a neither convex nor concave function of $\mathbf{q}_n$, which causes the non-convexity of constraints (13a), (13d) and (13e). Hence, problem (SP1-3) is non-convex, which is generally difficult to cope with. Nevertheless, we can use the SCA technique to transform non-convex constraints (13a), (13b), (13d) and (13e) to convex ones as follows.

For constraints (13a) and (13d), thanks to the special expression of $r_{i,n}$, we first relax $r_{i,n}$ by a concave lower-bound function. Based on Lemma 1, the following result holds true.

Lemma 2: For a given $\mathcal{Q}^t \triangleq \{\mathbf{q}_n^t\}$, $r_{i,n}$ can be lower bounded by $\tilde{r}_{i,n}$ with

$$\tilde{r}_{i,n} \triangleq a_{i,n} B \log_2 \left(1 + \frac{\Delta_2}{a_{i,n} z_{i,n}^t}\right) - \phi_{i,n}^t (z_{i,n} - z_{i,n}^t), \tag{14}$$

where $\Delta_2 = \frac{p_i \rho_0}{B N_0}$, $z_{i,n} = \max(\|\mathbf{q}_n - \mathbf{s}_i\|^2, d_{\min}^2)$, $z_{i,n}^t = \max(\|\mathbf{q}_n^t - \mathbf{s}_i\|^2, d_{\min}^2)$, and $\phi_{i,n}^t = \frac{a_{i,n} B \Delta_2}{z_{i,n}^t (a_{i,n} z_{i,n}^t + \Delta_2) \ln 2}$.

According to Lemma 3 in [37], we conclude $\tilde{r}_{i,n}$ is concave due to the convexity of $z_{i,n}$ with respect to $\mathbf{q}_n$ and $\phi_{i,n}^t > 0$. Via replacing $r_{i,n}$ by $\tilde{r}_{i,n}$ in constraints (13a) and (13d), these two constraints become convex.

As for the non-convex constraint (13e), we are going to replace $r_{i,n}$ by its convex upper approximation. Because of $\max(\|\mathbf{q}_n-\mathbf{s}_i\|^2, d_{\min}^2) \geqslant \|\mathbf{q}_n-\mathbf{s}_i\|^2$, we first obtain the upper bound $\breve{r}_{i,n}$ of $r_{i,n}$ with

$$\breve{r}_{i,n} = a_{i,n}B\log_2\left(1+\frac{\Delta_2}{a_{i,n}\|\mathbf{q}_n-\mathbf{s}_i\|^2}\right). \tag{15}$$

Since $\breve{r}_{i,n}$ is non-convex with respect to $\mathbf{q}_n$, we will find the convex upper bound of $\breve{r}_{i,n}$. We first show the related Hessian matrix.

Lemma 3: Denote $r_2(\mathbf{q}) = \log_2\left(1+\frac{c}{\|\mathbf{q}-\mathbf{s}\|^2}\right): \mathbb{R}^3 \to \mathbb{R}$, where c is a known positive constant and $\mathbf{s}\in\mathbb{R}^3$ is a known vector. Then for the Hessian matrix $\nabla^2\, r_2(\mathbf{q})$, it holds

$$\nabla^2 r_2(\mathbf{q}) \leqslant \frac{6c\|\mathbf{q}-\mathbf{s}\|^2+2c^2}{\|\mathbf{q}-\mathbf{s}\|^2(\|\mathbf{q}-\mathbf{s}\|^2+c)^2\ln 2}\mathbf{I}.$$

Proof: Define $f_1(z)=\log_2\left(1+\frac{c}{z}\right)$ and $f_2(\mathbf{q})=\|\mathbf{q}-\mathbf{s}\|^2$. Then it follows $r_2(\mathbf{q}) = f_1(f_2(\mathbf{q}))$. According to the chain rule [38], we can obtain

$$\begin{aligned}\nabla^2 r_2(\mathbf{q}) &= \nabla^2 f_1(f_2(\mathbf{q}))\cdot\nabla f_2(\mathbf{q})\cdot\nabla f_2(\mathbf{q})^T\\ &\quad+\nabla f_1(f_2(\mathbf{q}))\cdot\nabla^2\, f_2(\mathbf{q}).\end{aligned}$$

By taking the first and second order derivations of $f_1(z)$ and $f_2(\mathbf{q})$ respectively, one has

$$\nabla f_1(z) = -\frac{c}{z(z+c)\ln 2},\quad \nabla^2 f_1(z) = \frac{c(2z+c)}{z^2(z+c)^2\ln 2},$$

and

$$\nabla f_2(\mathbf{q}) = 2(\mathbf{q}-\mathbf{s}),\quad \nabla^2 f_2(\mathbf{q}) = 2\mathbf{I}.$$

Substituting above equations to $\nabla^2 r_2(\mathbf{q})$, it yields

$$\nabla^2 r_2(\mathbf{q}) = \frac{4c(2z+c)(\mathbf{q}-\mathbf{s})(\mathbf{q}-\mathbf{s})^T}{z^2(z+c)^2\ln 2} - \frac{2c}{z(z+c)\ln 2}\mathbf{I},$$

with $z=\|\mathbf{q}-\mathbf{s}\|^2$.

Matrix $\mathbf{\Lambda} = (\mathbf{q}-\mathbf{s})(\mathbf{q}-\mathbf{s})^T \in \mathbb{R}^3$ has only one nonzero eigenvalue, while other two eigenvalues are both zero. Moreover, for arbitrary two dimension compatible matrices $\mathbf{A}$ and $\mathbf{B}$, $\mathbf{AB}$ and $\mathbf{BA}$ admit the same nonzero eigenvalues. Thus, the eigenvalue vector of matrix $\mathbf{\Lambda}$ is $(\|\mathbf{q}-\mathbf{s}\|^2, 0, 0)^T$. Furthermore, the identity matrix $\mathbf{I}$ can be simultaneously diagonalized with arbitrary matrices, which implies the eigenvalues of $\nabla^2 r_2(\mathbf{q})$ are

$$\left(\frac{6cz+2c^2}{z(z+c)^2\ln 2}, -\frac{2c}{z(z+c)\ln 2}, -\frac{2c}{z(z+c)\ln 2}\right).$$

The proof is completed. ∎

Now we present the following theorem to show the convex upper bound of $r_{i,n}$.

Theorem 1: For a given trajectory $\mathbf{q}_n^t$, $r_{i,n}$ can be upper bounded by $\bar{r}_{i,n}$ with

$$\begin{aligned}\bar{r}_{i,n} &= a_{i,n}B\log_2\left(+\frac{\Delta_2}{a_{i,n}z_{i,n}^t}\right)\\ &\quad-\frac{2a_{i,n}B\Delta_2(\mathbf{q}_n^t-\mathbf{s}_i)^T(\mathbf{q}_n-\mathbf{q}_n^t)}{z_{i,n}^t(a_{i,n}z_{i,n}^t+\Delta_2)\ln 2}\\ &\quad+\frac{a_{i,n}B\Delta_2(3a_{i,n}z_{i,n}^t+\Delta_2)\|\mathbf{q}_n-\mathbf{q}_n^t\|^2}{z_{i,n}^t(a_{i,n}z_{i,n}^t+\Delta_2)^2\ln 2},\end{aligned} \tag{16}$$

where $\Delta_2=\frac{p_i\rho_0}{BN_0}$ and $z_{i,n}^t=\|\mathbf{q}_n^t-\mathbf{s}_i\|^2$. Moreover, $\bar{r}_{i,n}$ is convex with respect to $\mathbf{q}_n$.

Proof: As aforementioned, $\max(\|\mathbf{q}_n-\mathbf{s}_i\|^2, d_{\min}^2) \geqslant \|\mathbf{q}_n-\mathbf{s}_i\|^2$ leads to $r_{i,n}\leqslant\breve{r}_{i,n}$ with $\breve{r}_{i,n}$ defined in (15). In the sequel, we will show $\breve{r}_{i,n}\leqslant\bar{r}_{i,n}$.

For a function $f(x)$, its second-order Taylor expansion at the given point x_0 is expressed as

$$\begin{aligned}f(\mathbf{x}) &= f(\mathbf{x}_0)+\nabla f(\mathbf{x}_0)^T(\mathbf{x}-\mathbf{x}_0)\\ &\quad+\frac{(\mathbf{x}-\mathbf{x}_0)^T\nabla^2\, f(\mathbf{x}_0)(\mathbf{x}-\mathbf{x}_0)}{2}+o(\|\mathbf{x}-\mathbf{x}_0\|^2).\end{aligned}$$

If the Hessian matrix $\nabla^2 f(\mathbf{x}_0)$ is smaller than matrix $\mathbf{A}$, then we obtain

$$f(\mathbf{x})\leqslant f(\mathbf{x}_0)+\nabla f(\mathbf{x}_0)^T(\mathbf{x}-\mathbf{x}_0)+\frac{(\mathbf{x}-\mathbf{x}_0)^T\mathbf{A}(\mathbf{x}-\mathbf{x}_0)}{2}. \tag{17}$$

Regarding $\breve{r}_{i,n}$ as a function of $\mathbf{q}_n$ with $f(\mathbf{q}_n) = a_{i,n}B\log_2\left(1+\frac{\Delta_2}{a_{i,n}\|\mathbf{q}_n-\mathbf{s}_i\|^2}\right)$ and combining with Lemma 3, then it immediately follows from Eq. (17) that $\breve{r}_{i,n}\leqslant\bar{r}_{i,n}$ with $\bar{r}_{i,n}$ defined in (16). In addition, $\bar{r}_{i,n}$ is obviously convex with respect to $\mathbf{q}_n$. ∎

Based on the convexity of $\bar{r}_{i,n}$ in (16), replacing $r_{i,n}$ by $\bar{r}_{i,n}$ can transform the non-convex constraint (13e) to a convex one.

According to the above arguments, we turn to solve the approximate convex problem of problem (SP1-3) as follows:

$$\begin{aligned}(\text{SP1-4})\ &\max_{\eta,\mathcal{Q}}\quad \eta\\ &\text{s.t. } \frac{1}{N}\sum_{n\in\mathcal{N}}\tilde{r}_{i,n}\geqslant\eta,\quad\forall i, && (18a)\\ &\quad \mathbf{q}_0=\mathbf{q}_N, && (18b)\\ &\quad \|\mathbf{q}_{n+1}-\mathbf{q}_n\|^2\leqslant\delta^2V_{\max}^2,\quad\forall n, && (18c)\\ &\quad \sum_{n\leqslant N'}\sum_{i=1}^{N_k}\tilde{r}_{i,n}\delta\geqslant D^u(N'),\quad\forall N', && (18d)\\ &\quad \sum_{n\leqslant N'}\sum_{i=1}^{N_k}\bar{r}_{i,n}\delta\leqslant D^u(N')+C,\quad\forall N', && (18e)\end{aligned}$$

where $\tilde{r}_{i,n}$ and $\bar{r}_{i,n}$ are defined in (14) and (16), respectively.

We can utilize the CVX toolbox to solve problem (SP1-4) efficiently. Furthermore, due to $r_{i,n}\geqslant\tilde{r}_{i,n}$ and $r_{i,n}\leqslant\bar{r}_{i,n}$, the optimal solution of problem (SP1-4) is a lower bound of that of problem (SP1-3). We iteratively solve problem (SP1-4) multiple times to improve the quality of the solution. Following a similar analysis to Subsection IV-A, the iterations converge to a local minimum or a saddle point with a feasible starting point. Consequently, we can obtain the optimal trajectory with fixed bandwidth allocation.

In summary, for Area k, the bandwidth allocation and trajectory optimization is shown in Algorithm 1. Notably, when implementing Algorithm 1, giving the initial trajectory $\mathcal{Q}^{(0)}$ and bandwidth allocation $\mathcal{A}^{(0)}$ is necessary. We generate $\mathcal{Q}^{(0)}$ by the traveling salesman problem (TSP) based initial

Algorithm 1: IoT Bandwidth Allocation and UAV 3D Trajectory Design Algorithm

Input: Initial trajectory $\mathcal{Q}^{(0)}$ and bandwidth allocation $\mathcal{A}^{(0)}$, prescribed threshold ϵ_1, initial difference $\varphi^{(0)} = \epsilon_1 + 1$, iteration index $s = 0$.
Output: Optimal bandwidth allocation and trajectory $(\mathcal{A}^*, \mathcal{Q}^*)$.
1: **while** $\varphi^{(s)} \geqslant \epsilon_1$ **do**
2: Solve problem (SP1-2) to obtain $(\eta^{(s+1,1)}, \mathcal{A}^{(s+1)})$;
3: Solve problem (SP1-4) to obtain $(\eta^{(s+1)}, \mathcal{Q}^{(s+1)})$;
4: Compute the difference $\varphi^{(s+1)} = \frac{\eta^{(s+1)} - \eta^{(s)}}{\eta^{(s)}}$;
5: $s = s + 1$.
6: **end while**

trajectory design, which is detailedly presented in [21], [37] and thereby is omitted. For the initial bandwidth allocation $\mathcal{A}^{(0)}$, we can select $\mathcal{A}^{(0)}$ as a matrix with each element in $[0, 1]$ and the sum of each column being one. If the constraint (11e) is not satisfied, we can simultaneously shrink each element of $\mathcal{A}^{(0)}$ until it is met. Moreover, since the objective function value is not decreasing and upper bounded, Algorithm 1 can be convergent to the local optimal solution of problem (SP1) [21].

B. Sub-Problem 2: Power Allocation and Uplink Selection Optimization With Fixed Bandwidth Allocation and Trajectory

When the bandwidth allocation $\mathcal{A}_k$ and trajectory $\mathcal{Q}_k$ are fixed, by removing irrelevant terms with $(\mathcal{B}, \mathcal{P})$, IOP becomes

$$
\begin{aligned}
(\text{SP2}) \quad & \max_{\mathcal{B},\mathcal{P}} \quad \sum_{k\in\mathcal{K}} F_k \\
& \text{s.t. } P_{k,l,n} \geqslant 0, \quad \forall k, l, n, && (19a)\\
& \quad b_{k,l,n} P_{k,l,n} \leqslant P_{\max}, \quad \forall k, l, n, && (19b)\\
& \quad D_k^u(N') \leqslant D_k^r(N'), \quad \forall k, N' \in \mathcal{N}, && (19c)\\
& \quad D_k^u(N') \geqslant D_k^r(N') - C_k, \quad \forall k, N' \in \mathcal{N}, && (19d)\\
& \quad \sum_{k\in\mathcal{K}} b_{k,l,n} g(P_{k,l,n}, c_{k,l,n}) \leqslant R_{\max}, \quad \forall l, n, && (19e)\\
& \quad \sum_{l\in\mathcal{L}_n} b_{k,l,n} \leqslant 1, \quad \forall k, n, && (19f)\\
& \quad b_{k,l,n} \in \{0, 1\}, \quad \forall k, l, n. && (19g)
\end{aligned}
$$

Constraint (19b) is equivalent to (c7), and $D_k^r(N')$ is a known constant for any N' when $(\mathcal{A}_k, \mathcal{Q}_k)$ is fixed. Due to the coupled expression of $(\mathcal{B}, \mathcal{P})$ in the objective function as well as (19c)-(19e), together with the binary constraint in (19g), problem (SP2) is obviously not convex with respect to $(\mathcal{B}, \mathcal{P})$.

In order to cope with the non-convexity, we first introduce an auxiliary variable $\omega_{k,l,n} = g(P_{k,l,n}, c_{k,l,n})$. Then based on the definition of $g(p, c)$ in (3), we can express $P_{k,l,n}$ as a function of $\omega_{k,l,n}$ as follows:

$$
P_{k,l,n} = f(\omega_{k,l,n}) = \frac{2^{\frac{\omega_{k,l,n}}{W}} - 1}{\nu(c_{k,l,n})}, \tag{20}
$$

which is clearly a convex function of $\omega_{k,l,n}$. Clearly, $P_{k,l,n} \geqslant 0$ is equivalent to $\omega_{k,l,n} \geqslant 0$. Furthermore, let $\rho_{k,l,n} = b_{k,l,n}\omega_{k,l,n}$ and relax the inter programming constraint (19g) to a convex constraint $b_{k,l,n} \in [0, 1]$. Then according to the definition of $D_k^u(N')$ in Eq. (5) and definition of F_k in Eq. (9), with $\boldsymbol{\rho} = \{\rho_{k,l,n}\}$, we can approximate problem (SP2) by

$$
\begin{aligned}
(\text{SP2-1}) \max_{\mathcal{B},\boldsymbol{\rho}} \quad & \sum_{k\in\mathcal{K}} \sum_{n\in\mathcal{N}} \sum_{l\in\mathcal{L}_n} \delta \left[\rho_{k,l,n} - \beta b_{k,l,n} f\left(\frac{\rho_{k,l,n}}{b_{k,l,n}}\right)\right] \\
\text{s.t. } & \rho_{k,l,n} \geqslant 0, \quad \forall k, l, n, && (21a)\\
& b_{k,l,n} f\left(\frac{\rho_{k,l,n}}{b_{k,l,n}}\right) \leqslant P_{\max}, \quad \forall k, l, n, && (21b)\\
& \sum_{n\leqslant N'} \sum_{l\in\mathcal{L}_n} \rho_{k,l,n}\delta \leqslant D_k^r(N'), \quad \forall k, N', && (21c)\\
& \sum_{n\leqslant N'} \sum_{l\in\mathcal{L}_n} \rho_{k,l,n}\delta \geqslant D_k^r(N') - C_k, \quad \forall k, N', && (21d)\\
& \sum_{k\in\mathcal{K}} \rho_{k,l,n} \leqslant R_{\max}, \quad \forall l, n, && (21e)\\
& \sum_{l\in\mathcal{L}_n} b_{k,l,n} \leqslant 1, \quad \forall k, n, && (21f)\\
& b_{k,l,n} \in [0, 1], \quad \forall k, l, n. && (21g)
\end{aligned}
$$

To begin with, we claim the convexity of problem (SP2-1).

Proposition 1: Problem (SP2-1) is convex.

Proof: For $b > 0$, we denote function $\Upsilon(b, \rho) = bf(\frac{\rho}{b})$ with $f(\cdot)$ given by (20) and $\rho \geqslant 0$. By taking the second order derivative of $\Upsilon(b, \rho)$ with respect to (b, ρ), we obtain

$$
\nabla^2\Upsilon(b, \rho) = \frac{\nabla^2 f(\frac{\rho}{b})}{b^3} \begin{pmatrix} b^2 & -b\rho \\ -b\rho & \rho^2 \end{pmatrix}.
$$

Since $f(\cdot)$ is a convex function, it holds $\nabla^2 f(\frac{\rho}{b}) \geqslant 0$. Then, it yields $\nabla^2\Upsilon(b, \rho) \geqslant 0$, which means that $b_{k,l,n} f\left(\frac{\rho_{k,l,n}}{b_{k,l,n}}\right)$ is convex with respect to $(\mathcal{B}, \boldsymbol{\rho})$. Therefore, the objective function in problem (SP2-1) is concave while all constraints are convex, which leads to the convexity of problem (SP2-1). ∎

Inspired by [25], we adopt the Lagrangian dual decomposition method to get the optimal solution of problem (SP2-1).

1) Lagrangian Dual Decomposition Method: By introducing nonnegative Lagrangian multipliers $\boldsymbol{\lambda} = \{\lambda_{k,l,n}\}$, $\boldsymbol{\gamma} = \{\gamma_{k,N'}\}$, $\boldsymbol{\mu} = \{\mu_{k,N'}\}$, $\boldsymbol{\xi} = \{\xi_{l,n}\}$, $\boldsymbol{\theta} = \{\theta_{k,n}\}$ associated with corresponding constraints (21b)-(21f), respectively, we formulate the Lagrangian function by

$$
\begin{aligned}
& \boldsymbol{L}\ (\mathcal{B}, \boldsymbol{\rho}, \boldsymbol{\lambda}, \boldsymbol{\mu}, \boldsymbol{\gamma}, \boldsymbol{\xi}, \boldsymbol{\theta}) \\
& = \sum_{k\in\mathcal{K}} \sum_{n\in\mathcal{N}} \sum_{l\in\mathcal{L}_n} \delta \left[\rho_{k,l,n} - \beta b_{k,l,n} f\left(\frac{\rho_{k,l,n}}{b_{k,l,n}}\right)\right] \\
& \quad + \sum_{k\in\mathcal{K}} \sum_{n\in\mathcal{N}} \sum_{l\in\mathcal{L}_n} \lambda_{k,l,n} \left[P_{\max} - b_{k,l,n} f\left(\frac{\rho_{k,l,n}}{b_{k,l,n}}\right)\right] \\
& \quad + \sum_{N'\in\mathcal{N}} \sum_{k\in\mathcal{K}} \gamma_{k,N'} \Big(D_k^r(N') - \sum_{n\leqslant N'} \sum_{l\in\mathcal{L}_n} \rho_{k,l,n}\delta \Big) \\
& \quad + \sum_{N'\in\mathcal{N}} \sum_{k\in\mathcal{K}} \mu_{k,N'} \Big(\sum_{n\leqslant N'} \sum_{l\in\mathcal{L}_n} \rho_{k,l,n}\delta - D_k^r(N') + C_k \Big) \\
& \quad + \sum_{n\in\mathcal{N}} \sum_{l\in\mathcal{L}_n} \xi_{l,n} (R_{\max} - \sum_{k\in\mathcal{K}} \rho_{k,l,n})
\end{aligned}
$$

$$+\sum_{k\in\mathcal{K}}\sum_{n\in\mathcal{N}}\theta_{k,n}(1-\sum_{l\in\mathcal{L}_n}b_{k,l,n}).$$

Notice that, constraints (21a) and (21g) are not involved in the Lagrangian function.

The dual function is

$$\mathcal{G}(\boldsymbol{\lambda},\boldsymbol{\gamma},\boldsymbol{\mu},\boldsymbol{\xi},\boldsymbol{\theta})=\max_{(21a),(21g)}\boldsymbol{L}(\mathcal{B},\boldsymbol{\rho},\boldsymbol{\lambda},\boldsymbol{\gamma},\boldsymbol{\mu},\boldsymbol{\xi},\boldsymbol{\theta}). \quad (22)$$

Then the Lagrangian dual problem is given by

$$\min_{\boldsymbol{\lambda},\boldsymbol{\gamma},\boldsymbol{\mu},\boldsymbol{\xi},\boldsymbol{\theta}} \quad \mathcal{G}(\boldsymbol{\lambda},\boldsymbol{\gamma},\boldsymbol{\mu},\boldsymbol{\xi},\boldsymbol{\theta})$$
$$\text{s.t. } \boldsymbol{\lambda},\boldsymbol{\gamma},\boldsymbol{\mu},\boldsymbol{\xi},\boldsymbol{\theta}\geqslant 0.$$

We first deduce how to determine the optimal $(\rho^*_{k,l,n},b^*_{k,l,n})$ with given Lagrangian multipliers $(\boldsymbol{\lambda},\boldsymbol{\gamma},\boldsymbol{\mu},\boldsymbol{\xi},\boldsymbol{\theta})$, $\forall k,l,n$.

Since problem (SP2-1) is convex with respect to $(\mathcal{B},\boldsymbol{\rho})$, taking the constraint $\rho_{k,l,n}\geqslant 0$ in (21a) into account, the optimal solution $\rho^*_{k,l,n}$ should satisfy the condition

$$\begin{cases}\rho^*_{k,l,n}=0, & \text{if } \dfrac{\partial \boldsymbol{L}}{\partial\rho_{k,l,n}}|_{\rho_{k,l,n}=0}<0,\\ \dfrac{\partial \boldsymbol{L}}{\partial\rho_{k,l,n}}|_{\rho_{k,l,n}=\rho^*_{k,l,n}}=0, & \text{otherwise,}\end{cases} \quad (23)$$

where $\frac{\partial \boldsymbol{L}}{\partial\rho_{k,l,n}}$ is the partial derivative of $\boldsymbol{L}$ with respect to $\rho_{k,l,n}$. It is not difficult to compute

$$\frac{\partial \boldsymbol{L}}{\partial\rho_{k,l,n}}=\delta-\frac{(\delta\beta+\lambda_{k,l,n})(\ln 2)2^{\frac{\rho_{k,l,n}}{Wb_{k,l,n}}}}{W\nu(c_{k,l,n})}+\delta\sum_{N'\geqslant n}(\mu_{k,N'}-\gamma_{k,N'})-\xi_{l,n}.$$

Then by the optimal condition Eq. (23), we can obtain

$$\rho^*_{k,l,n}=\max\left\{0,b_{k,l,n}W\log_2\frac{W\nu(c_{k,l,n})\Delta}{(\delta\beta+\lambda_{k,l,n})\ln 2}\right\} \quad (24)$$

with $\Delta=\delta-\xi_{l,n}+\delta\sum_{N'\geqslant n}(\mu_{k,N'}-\gamma_{k,N'})$. Recalling the transformation $\rho_{k,l,n}=b_{k,l,n}\omega_{k,l,n}$, it immediately holds

$$\omega^*_{k,l,n}=\max\left\{0,W\log_2\frac{W\nu(c_{k,l,n})\Delta}{(\delta\beta+\lambda_{k,l,n})\ln 2}\right\}. \quad (25)$$

According to expression $P_{k,l,n}=f(\omega_{k,l,n})$ in Eq. (20), we further get the optimal solution $P^*_{k,l,n}$ for problem (SP2) as

$$P^*_{k,l,n}=\frac{2^{\frac{\omega^*_{k,l,n}}{W}}-1}{\nu(c_{k,l,n})}. \quad (26)$$

Using a similar argument and considering the constraint $b_{k,l,n}\in[0,1]$ in (21g), the optimal solution $b^*_{k,l,n}$ is given by

$$\begin{cases}b^*_{k,l,n}=0, & \text{if } \dfrac{\partial \boldsymbol{L}}{\partial b_{k,l,n}}|_{b_{k,l,n}=0}<0,\\ b^*_{k,l,n}\in(0,1), & \text{if } \dfrac{\partial \boldsymbol{L}}{\partial b_{k,l,n}}|_{b^*_{k,l,n}}=0,\\ b^*_{k,l,n}=1, & \text{if } \dfrac{\partial \boldsymbol{L}}{\partial b_{k,l,n}}|_{b_{k,l,n}=1}>0,\end{cases} \quad (27)$$

where $\frac{\partial \boldsymbol{L}}{\partial b_{k,l,n}}$ is the partial derivative of $\boldsymbol{L}$ with respect to $b_{k,l,n}$. We can easily derive

$$\frac{\partial \boldsymbol{L}}{\partial b_{k,l,n}}=\frac{(\delta\beta+\lambda_{k,l,n})((\omega_{k,l,n}\ln 2-W)2^{\frac{\omega_{k,l,n}}{W}}+W)}{W\nu(c_{k,l,n})}-\theta_{k,n}.$$

As can be seen from the above expression, when $\omega^*_{k,l,n}$ in Eq. (25) is determined, $\frac{\partial \boldsymbol{L}}{\partial b_{k,l,n}}$ is a constant with uncertain sign. When $\frac{\partial \boldsymbol{L}}{\partial b_{k,l,n}}<0$ does not hold for all l, there exist at least one index l such that $b_{k,l,n}>0$. In this case, due to $b_{k,l,n}\in\{0,1\}$ in problem (SP2) and $\sum_{l\in\mathcal{L}_n}b_{k,l,n}\leqslant 1$, i.e., one UAV is supposed to transmit data to at most one LEO satellite at one time slot, we obtain the optimal solution $b^*_{k,l,n}$ for problem (SP2) as

$$b_{k,l^*,n}=1 \quad \text{with} \quad l^*=\arg\max_l\frac{\partial \boldsymbol{L}}{\partial b_{k,l,n}}. \quad (28)$$

2) Update of Lagrangian Multipliers: Because the Lagrangian dual function in (22) may be non-differentiable, the subgradient method is used to update the Lagrangian multipliers $(\boldsymbol{\lambda},\boldsymbol{\mu},\boldsymbol{\gamma},\boldsymbol{\xi},\boldsymbol{\theta})$ [39]. It is not difficult to deduce the subgradient of $\boldsymbol{L}$ with respect to $(\boldsymbol{\lambda},\boldsymbol{\mu},\boldsymbol{\xi},\boldsymbol{\theta})$ are respectively

$$\begin{aligned}\frac{\partial \boldsymbol{L}}{\partial\lambda_{k,l,n}}&=P_{\max}-b_{k,l,n}f\left(\frac{\rho_{k,l,n}}{b_{k,l,n}}\right),\\ \frac{\partial \boldsymbol{L}}{\partial\gamma_{k,N'}}&=D^r_k(N')-\sum_{n\leqslant N'}\sum_{l\in\mathcal{L}_n}\rho_{k,l,n}\delta,\\ \frac{\partial \boldsymbol{L}}{\partial\mu_{k,N'}}&=\sum_{n\leqslant N'}\sum_{l\in\mathcal{L}_n}\rho_{k,l,n}\delta-D^r_k(N')+C_k,\\ \frac{\partial \boldsymbol{L}}{\partial\xi_{l,n}}&=R_{\max}-\sum_{k\in\mathcal{K}}\rho_{k,l,n},\\ \frac{\partial \boldsymbol{L}}{\partial\theta_{k,n}}&=1-\sum_{l\in\mathcal{L}_n}b_{k,l,n}.\end{aligned}$$

Then, we update the Lagrangian multipliers as follows

$$\lambda^{(s+1)}_{k,l,n}=\left[\lambda^{(s)}_{k,l,n}-\tau^{(s)}_1\left(P_{\max}-b_{k,l,n}f\left(\frac{\rho_{k,l,n}}{b_{k,l,n}}\right)\right)\right]^+, \quad (29)$$

$$\gamma^{(s+1)}_{k,N'}=\left[\gamma^{(s)}_{k,N'}-\tau^{(s)}_2\Big(D^r_k(N')-\sum_{n\leqslant N'}\sum_{l\in\mathcal{L}_n}\rho_{k,l,n}\delta\Big)\right]^+, \quad (30)$$

$$\mu^{(s+1)}_{k,N'}=\left[\mu^{(s)}_{k,N'}-\tau^{(s)}_3\Big(\sum_{n\leqslant N'}\sum_{l\in\mathcal{L}_n}\rho_{k,l,n}\delta-D^r_k(N')+C_k\Big)\right]^+, \quad (31)$$

$$\xi^{(s+1)}_{l,n}=\left[\xi^{(s)}_{l,n}-\tau^{(s)}_4(R_{\max}-\sum_{k\in\mathcal{K}}\rho_{k,l,n})\right]^+, \quad (32)$$

$$\theta^{(s+1)}_{k,n}=\left[\theta^{(s)}_{k,n}-\tau^{(s)}_5(1-\sum_{l\in\mathcal{L}_n}b_{k,l,n})\right]^+, \quad (33)$$

where s is the iteration index, $\boldsymbol{\tau}=\{\tau_1,\ldots,\tau_5\}$ represents the step size, and the notation $[\cdot]^+$ means $\max\{0,\cdot\}$. Therefore,

Algorithm 2: UAV Power Allocation and LEO Satellite Selection Algorithm

Input: Initial Lagrangian multipliers $\boldsymbol{\lambda}^{(0)}$, $\boldsymbol{\gamma}^{(0)}$, $\boldsymbol{\mu}^{(0)}$, $\boldsymbol{\xi}^{(0)}$, $\boldsymbol{\theta}^{(0)}$, prescribed threshold ϵ_2, initial difference $\phi^{(0)} = \epsilon_2 + 1$, step size $\{\boldsymbol{\tau}\}$, iteration index $s = 0$.

Output: Optimal power allocation and uplink selection policy $(\mathcal{B}^*, \mathcal{P}^*)$.

1: **while** $\phi^{(s)} \geqslant \epsilon_2$ **do**
2: Use (25) and (26) to obtain the optimal power allocation $\mathcal{P}^{s+1}$;
3: Use (27) and (28) to obtain the optimal uplink selection $\mathcal{B}^{s+1}$;
4: Use (29), (30), (31), (32), (33) to update multipliers $\boldsymbol{\lambda}^{(s+1)}, \boldsymbol{\gamma}^{(s+1)}, \boldsymbol{\mu}^{(s+1)}, \boldsymbol{\xi}^{(s+1)}, \boldsymbol{\theta}^{(s+1)}$;
5: Compute the difference $\phi^{(s+1)} = \frac{\|\boldsymbol{\lambda}^{(s+1)} - \boldsymbol{\lambda}^{(s)}\|}{\|\boldsymbol{\lambda}^{(s)}\|} + \frac{\|\boldsymbol{\gamma}^{(s+1)} - \boldsymbol{\gamma}^{(s)}\|}{\|\boldsymbol{\gamma}^{(s)}\|} + \frac{\|\boldsymbol{\mu}^{(s+1)} - \boldsymbol{\mu}^{(s)}\|}{\|\boldsymbol{\mu}^{(s)}\|} + \frac{\|\boldsymbol{\xi}^{(s+1)} - \boldsymbol{\xi}^{(s)}\|}{\|\boldsymbol{\xi}^{(s)}\|} + \frac{\|\boldsymbol{\theta}^{(s+1)} - \boldsymbol{\theta}^{(s)}\|}{\|\boldsymbol{\theta}^{(s)}\|}$;
6: $s = s + 1$.
7: **end while**

the power allocation and uplink selection optimization is shown in Algorithm 2.

Since the subgradients are bounded, if $\{\boldsymbol{\tau}^{(s)}\}$ is generated by a diminishing step-size rule, i.e.,

$$\sum_{s=1}^{\infty} \boldsymbol{\tau}^{(s)} = \infty, \quad \lim_{s \to \infty} \boldsymbol{\tau}^{(s)} = 0,$$

the multiplier sequence $\{(\boldsymbol{\lambda}^{(s)}, \boldsymbol{\gamma}^{(s)}, \boldsymbol{\mu}^{(s)}, \boldsymbol{\xi}^{(s)}, \boldsymbol{\theta}^{(s)})\}$ generated by Algorithm 2 is convergent to the optimal value [40]. In addition, the primal variables $(\mathcal{B}^s, \mathcal{P}^s)$ are updated in an analytical form, and thereby the convergence rate mainly relies on the optimization of the dual variables. Since the optimization of dual variables is based on the subgradient method, we can speed up the convergence by adopting the adaptive step size

$$\tau_i{}^{(s)} = \frac{1}{\sqrt{s}}, \quad i = 1, \ldots, 5.$$

Consequently, based on the above analyses, we can obtain the optimal power allocation and uplink selection.

C. BCD Based Approach for IOP and Computational Complexity

In Subsections IV-A and IV-B, we propose Algorithms 1 and 2 to solve sub-problems (SP1) and (SP2), respectively. To jointly optimize the bandwidth allocation, trajectory, power allocation and uplink selection, on basis of obtained solutions of sub-problems (SP1) and (SP2), we implement the BCD process as follows. With fixed power allocation and uplink selection $(\mathcal{B}, \mathcal{P})$, we apply Algorithm 1 to optimize $(\mathcal{A}_k, \mathcal{Q}_k)$, $k = 1, \ldots, K$. Then with obtained $(\mathcal{A}_k, \mathcal{Q}_k)$, we adopt Algorithm 2 to solve $(\mathcal{A}_k, \mathcal{Q}_k)$. Algorithms 1 and 2 are alternatively executed until the objective function value of IOP changes in a prescribed threshold. The BCD based approach can converge to at least a locally optimal solution of IOP following the analysis similar to [21].

The computational complexity of the BCD based approach for IOP mainly depends on those of Algorithms 1 and 2. For Algorithm 1, it involves solving convex problems (SP1-2) and (SP1-4), where their variable numbers are $MN + K$ and $3M + K$, respectively. By employing a primal-dual interior point method to solve problems (SP1-2) and (SP1-4), the computation complexities are respectively $O((MN + K)^3 \log(\epsilon^{-1}))$ and $O((3M + K)^3 \log(\epsilon^{-1}))$ with ϵ being the accepted duality gap. Supposing that the number of iterations in Algorithm 1 is S_1, then the total computation complexity for Algorithm 1 can be calculated as $O\left(S_1((MN + K)^3 + (3M + K)^3) \log(\epsilon^{-1})\right)$. For Algorithm 2, since an analytical iteration is performed in each step, assuming that the total iterative number is S_2, then computation complexity for Algorithm 2 is $O(S_2 KLN)$. Therefore, given the total iteration number S of the BCD based approach for IOP, its total computational complexity is formulated as $O\left(SS_1((MN + K)^3 + (3M + K)^3) \log(\epsilon^{-1}) + SS_2 KLN\right)$.

V. Numerical Simulations

In this section, numerous simulations are carried out to validate the effectiveness of the proposed BCD based approach for IOP.

Assume that a mountain region under surveillance with 50 km $\times$ 50 km is divided into $K = 10$ areas which are far apart from each other. In each area, a single UAV gathers data from $N_k = 10$ IoT devices, $k = 1, \ldots, 10$. In addition, these IoT devices within each area are randomly and dependently distributed in a polyhedron area with height 100 m, while the lengths in Areas 1-2, 3-5, 6-8, 9-10 are respectively 2000 m, 3000 m, 4000 m and 5000 m. Meanwhile, there are $L_n = L = 5$ LEO satellites in the air that can simultaneously receive data from UAVs of these K areas, $n = 1, \ldots, N$. The maximum receiving rate of LEO satellite $R_{\max}$ is set to 10 Mbits/s. The weight coefficient β is selected as 0.5. When optimizing the objective function $F_k = D_k^{tu} - \beta E_k$ in problem (SP2), we modify $F_k = D_k^{tu} - 10^6 \beta E_k$ by taking the magnitudes of D_k^{tu} and E_k into account. We assume that the appointed mission period T is $T = 100$ s. As mentioned behind Eq. (3), during the mission period T, the fading coefficient $\nu(c_{k,l,n})$ is randomly generated from 5.03, 3.46, and 1.0, $k = 1, \ldots, 10$, $l = 1, \ldots, 5$. Other main parameters of our numerical simulations are set in Table II.

With the above setup, we first display the trajectory and LEO satellite selection of UAVs in Areas 1-10 in Fig. 2(a), where the selection situation corresponds to the first time slot. As shown in Fig. 2(a), at the first time slot, UAVs U_2, U_7, and U_8 transmit data to LEO 1, UAV U_5 has the uplink with LEO 2, UAVs U_1 and U_9 transmit data to LEO 3, UAVs U_3, U_4 and U_{10} transmit data to LEO 4, while UAV U_6 has the uplink with LEO 5. In order to show the trajectory more clearly, we plot Area 1 as an example in Fig. 2(b). With the TSP based initial trajectory, we can obtain the optimal 3D trajectory. Since the appointed time is shorter than its TSP

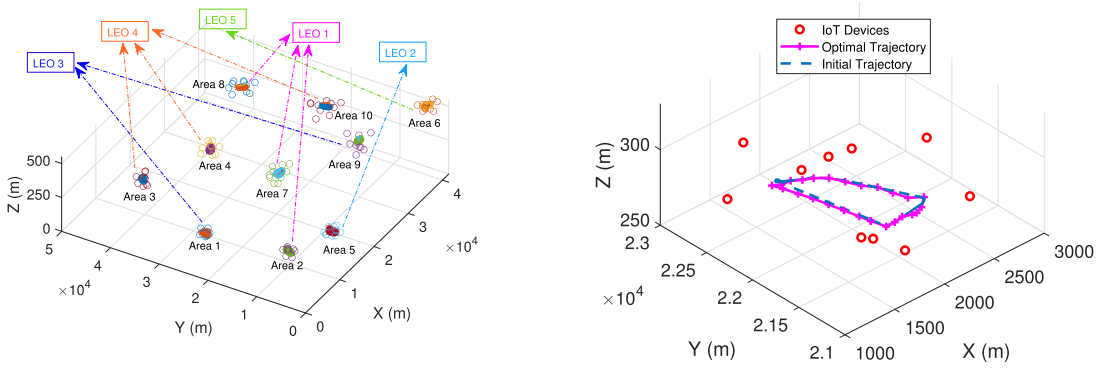

Fig. 2. Optimal trajectory of UAVs: (a) Trajectory of all areas and LEO satellite selection; (b) Trajectory of area 1.

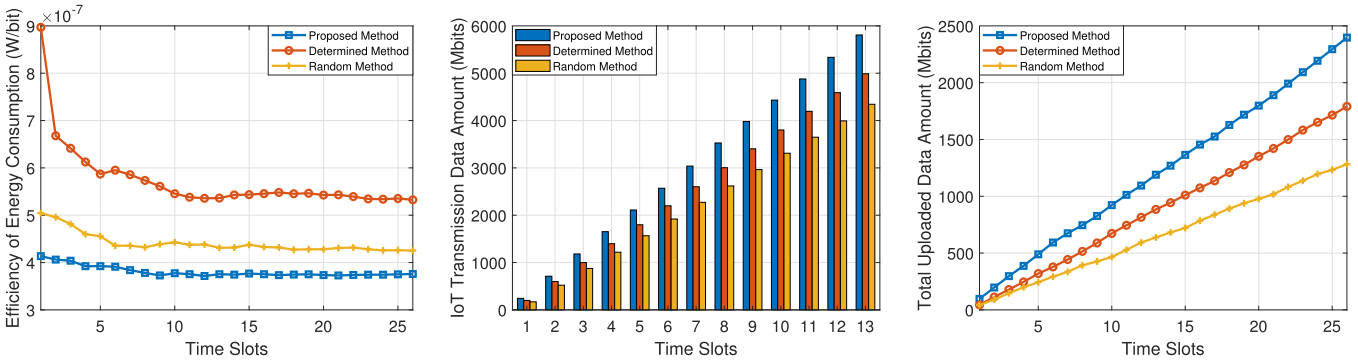

Fig. 3. Performance comparison of three methods: (a) Efficiency of energy consumption (W/bit); (b) IoT transmission data amount (Mbits); (c) Total uploaded data amount of UAVs (Mbits).

TABLE II
MAIN SIMULATION PARAMETERS

Parameter	Value
Time slot length: δ	4 s
Safe distance between UAVs and IoT devices: $d_{\min}$	30 m
Channel power gain at reference distance of $d_0 = 1$ m: ρ_0	-50 dB
Total available bandwidth for each UAV B	1 MHz
Transmit power of $I_{i,k}$: $p_{i,k}$	0.01 W
AWGN power spectral density N_0	-169 dBm/Hz
Bandwidth of UAV transmission to LEO satellites: W	1 MHz
Maximum speed of UAV: $V_{\max}$	30 m/s
Maximum transmit power of UAV: $P_{\max}$	1 W
Cache capacity of UAV C_k	500 Mbits
Thresholds in Algorithms 1 and 2: ϵ_1, ϵ_2	10^{-3}

time, the UAV cannot arrive at each IoT device in this area. Work [37] has shown that the obtained 3D trajectory admits better performance than the 2D trajectory.

To the best of our knowledge, there was no algorithm for solving IOP. In order to evaluate the performance of the proposed algorithm, we compare it with two benchmark methods: determined method and random method. For the determined method, the total bandwidth of the UAV is equally allocated to all IoT devices in each area, the trajectory of the UAV is set to be the TSP based initial trajectory, each UAV select the LEO satellite which admits the best channel condition, and the transmission rate of each UAV is the same while the total received rate of each LEO satellite is just equal to $R_{\max}$. For the determined method, when the constraints (c8) and (c9) in IOP are not satisfied, the bandwidth allocated to each IoT device and the transmission rate of each UAV will shrink until the two constraints hold. For the random method, we randomly generate the bandwidth allocation, randomly select the LEO satellites and randomly give the transmit power of each UAV until the constraints (c8) and (c9) are met, and the trajectory of the UAV still adopts the TSP based initial trajectory. When characterizing the algorithm performance, we use the efficiency of energy consumption of UAVs, the IoT transmission data amount, and total uploaded data amount by UAVs as metrics. Here the efficiency of energy consumption of UAV k is defined by the ratio of its energy consumption on uploading data to LEO satellites and its uploaded data amount as E_k/D_k^{tu}, where E_k and D_k^{tu} are the energy consumption given by (8) and the uploaded data amount given by (4), respectively. Without UAV backlogs, the lower the efficiency of energy consumption and the larger the IoT transmission data amount and total uploaded data amount, the better performance the method admits.

Then we depict the efficiency of energy consumption, IoT transmission data amount, and total uploaded data amount with respect to time slots for the proposed method, determined method and random method in Fig. 3. It is easy to see, the efficiencies of energy consumption of the proposed method

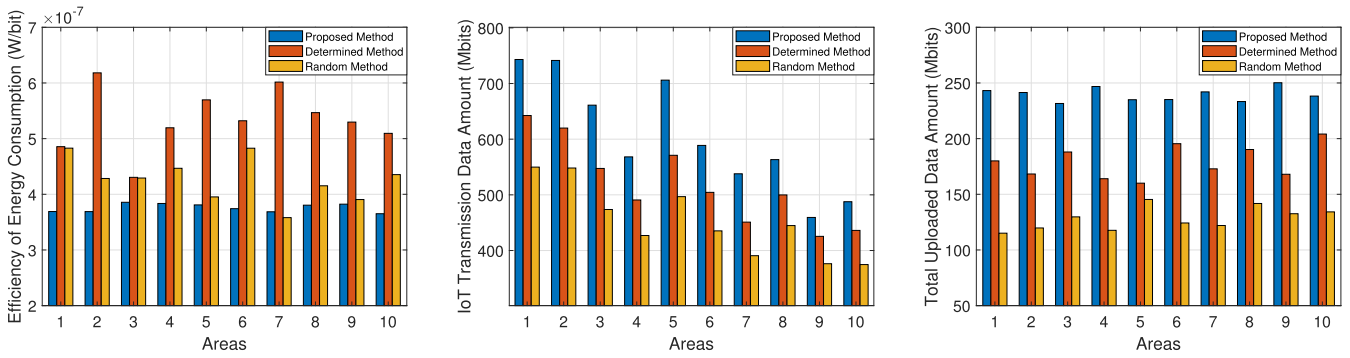

Fig. 4. Performance comparison of 10 areas: (a) Efficiency of energy consumption (W/bit); (b) IoT transmission data amount (Mbits); (c) Total uploaded data amount of UAVs (Mbits).

differ small during all the time slots, which implies they are balanced in each time slot. With the increase of time slots, both the IoT transmission data amount and the total uploaded data amount of UAVs are increasing nearly in a linear trend. Obviously, the proposed method is superior to the other two methods in all the three aspects. As can be seen from Fig. 3, our method has a much lower efficiency of energy consumption and much larger uploaded data amount. Therefore, our method admits better performance.

Moreover, since the IoT device densities in Area 1-Area 10 are not all the same, we compare efficiency of energy consumption, IoT transmission data amount, and total uploaded data amount of UAVs in Areas 1-10. Recalling that the lengths in Areas 1-2, 3-5, 6-8, 9-10 are respectively 2000 m, 3000 m, 4000 m and 5000 m, the IoT device densities in Areas 1-2, 3-5, 6-8, 9-10 are decreasing. From Figs. 4(a) and 4(c), the efficiency of energy consumption and the total uploaded data amount have no obvious trend for these three methods, whereas the IoT transmission data amount of the three methods have a decreasing trend for Areas 1-2, 3-5, 6-8, 9-10 in Fig. 4(b). Because the smaller IoT device density leads to larger distances among 10 IoT devices, the data amount gathered by UAV will decrease in a same time period. On the other hand, since the 10 UAVs in each area transmit data to LEO satellites collaboratively, the total uploaded data amount as well as the efficiency of energy consumption does not differ greatly in areas.

In the following, we will show how the maximum receiving rate $R_{\max}$ and the number of LEO satellites L affect the proposed method. We consider the scenario that the length of each area is equal to 5000 m, and the time slot length is set to 5 s. Other simulation parameters keep unchanged.

1) Comparison of Different Maximum Receiving Rate $R_{\max}$: In order to illustrate the effect of the maximum receiving rate $R_{\max}$ of LEO satellites, we compare eight cases with $R_{\max} = \{1, 3, 5, 7, 9, 11, 13, 15\}$ Mbits/s, respectively. As shown in Figs. 5 and 6, for all these eight cases, the proposed method performs better than the determined method and the random method in terms of both the efficiency of energy consumption and the total uploaded data amount, while the determined method and the random method have no clear superiority to each other. Moreover, when $R_{\max}$ becomes

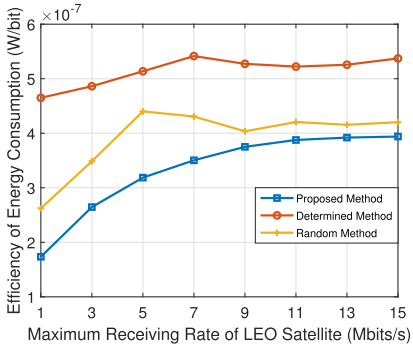

Fig. 5. Efficiency of energy consumption with different $R_{\max}$.

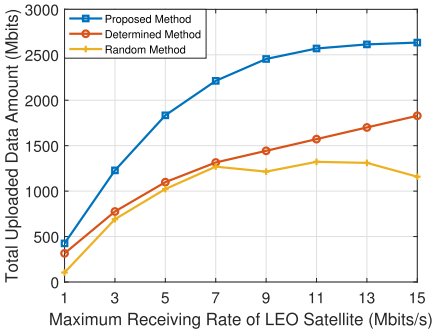

Fig. 6. Total uploaded data amount with different $R_{\max}$.

larger, the LEO satellites can receive more data at each time slot, which leads to larger total uploaded data amount. However, the efficiency of energy consumption becomes worse with larger $R_{\max}$. In addition, when $R_{\max}$ exceeds a certain threshold (about 11 Mbits/s for this example), the gain in uploaded data amount almost disappears. Actually, by only adding $R_{\max}$ to a certain value, the IoT transmission data will not change any longer, which further causes that the uploaded data amount nearly keeps unchanged. Therefore, we can use different LEO satellites with proper maximum receiving rate $R_{\max}$ rather than a large one in practical applications.

2) Comparison of Different Numbers of LEO Satellites L: When the number of LEO satellites L varies in $L = \{1, 2, 3, 4, 5\}$, we show the efficiency of energy consumption

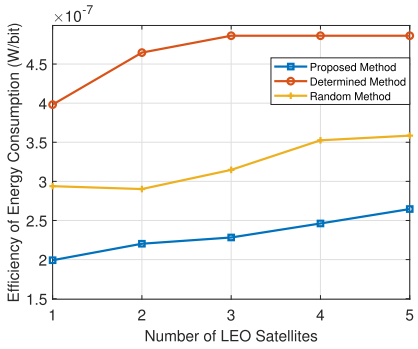

Fig. 7. Efficiency of energy consumption with different L.

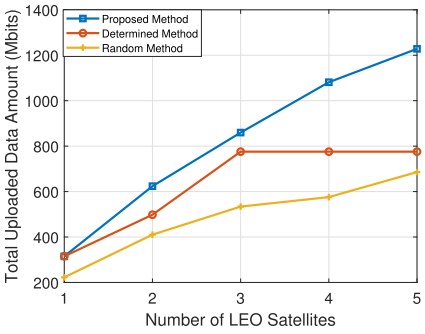

Fig. 8. Total uploaded data amount with different L.

and total uploaded data amount in Figs. 7 and 8, respectively. It is easy to see, the proposed method outperforms the other two methods. Meanwhile, the total uploaded data amount is increasing with respect to L, as shown in Fig. 8. When L becomes larger, UAVs have more chances to select the LEO satellite with better channel state. Meanwhile, with the increase of L, the LEO satellite constellation possesses more data receiving capacity. However, the efficiency of energy consumption becomes slightly worse with respect to L. In practical applications, we can adjust the number of LEO satellites to satisfy different preference on energy consumption or uploaded data amount.

VI. Conclusion and Future Work

In this paper, we have investigated a UAV-LEO integrated data collection in the B5G IoRT networks. Specifically, to maximize the total uploaded data amount to LEO satellites and minimize the energy consumption of UAVs simultaneously, we have proposed a BCD-based method to jointly optimize the IoT bandwidth allocation, UAV 3D trajectory design, UAV power allocation and LEO satellite selection. Numerical results have shown the superiority and effectiveness of the proposed method. The work could provide useful guidelines for deployment and data collection algorithm design in B5G IoRT networks. For the future work, we will consider the dynamic interconnection and transmission optimization among satellites for massive LEO satellite networking to provide better data collection sevices in B5G IoRT networks.

References

[1] W. Saad, M. Bennis, and M. Chen, "A vision of 6G wireless systems: Applications, trends, technologies, and open research problems," *IEEE Netw.*, vol. 34, no. 3, pp. 134–142, May 2020.

[2] N. Cheng *et al.*, "Air-ground integrated mobile edge networks: Architecture, challenges, and opportunities," *IEEE Commun. Mag.*, vol. 56, no. 8, pp. 26–32, Aug. 2018.

[3] N. Cheng *et al.*, "A comprehensive simulation platform for space-air-ground integrated network," *IEEE Wireless Commun.*, vol. 27, no. 1, pp. 178–185, Feb. 2020.

[4] J. Liu, Y. Shi, Z. M. Fadlullah, and N. Kato, "Space-air-ground integrated network: A survey," *IEEE Commun. Surveys Tuts.*, vol. 20, no. 4, pp. 2714–2741, 2018.

[5] M. De Sanctis, E. Cianca, G. Araniti, I. Bisio, and R. Prasad, "Satellite communications supporting Internet of remote things," *IEEE Internet Things J.*, vol. 3, no. 1, pp. 113–123, Feb. 2016.

[6] Z. Li *et al.*, "Energy efficient resource allocation for UAV-assisted space-air-ground Internet of remote Things networks," *IEEE Access*, vol. 7, pp. 145348–145362, 2019.

[7] B. Qian, H. Zhou, T. Ma, K. Yu, Q. Yu, and X. Shen, "Multi-operator spectrum sharing for massive IoT coexisting in 5G/B5G wireless networks," *IEEE J. Sel. Areas Commun.*, vol. 39, no. 3, pp. 881–895, Mar. 2020.

[8] Z. Qu, G. Zhang, H. Cao, and J. Xie, "LEO satellite constellation for Internet of Things," *IEEE Access*, vol. 5, pp. 18391–18401, 2017.

[9] Z. Jia, M. Sheng, J. Li, D. Niyato, and Z. Han, "LEO-satellite-assisted UAV: Joint trajectory and data collection for Internet of remote things in 6G aerial access networks," *IEEE Internet Things J.*, vol. 8, no. 12, pp. 9814–9826, Jun. 2020.

[10] S.-Y. Lien, K.-C. Chen, and Y. Lin, "Toward ubiquitous massive accesses in 3GPP machine-to-machine communications," *IEEE Commun. Mag.*, vol. 49, no. 4, pp. 66–74, Apr. 2011.

[11] Global Industry Analysis, Inc. (Jul. 2020). *UAV Drones-Global Market Trajectory & Analytics*. [Online]. Available: https://www.researchandmarkets.com/reports/4806222

[12] W. Shi *et al.*, "Multi-drone 3-D trajectory planning and scheduling in drone-assisted radio access networks," *IEEE Trans. Veh. Technol.*, vol. 68, no. 8, pp. 8145–8158, Aug. 2019.

[13] W. Shi, H. Zhou, J. Li, W. Xu, N. Zhang, and X. Shen, "Drone assisted vehicular networks: Architecture, challenges and opportunities," *IEEE Netw.*, vol. 32, no. 3, pp. 130–137, May 2018.

[14] Q. Wu and R. Zhang, "Common throughput maximization in UAV-enabled OFDMA systems with delay consideration," *IEEE Trans. Commun.*, vol. 66, no. 12, pp. 6614–6627, Dec. 2018.

[15] M. A. Ali, Y. Zeng, and A. Jamalipour, "Software-defined coexisting UAV and WiFi: Delay-oriented traffic offloading and UAV placement," *IEEE J. Sel. Areas Commun.*, vol. 38, no. 6, pp. 988–998, Jun. 2020.

[16] Y. Zeng, Q. Wu, and R. Zhang, "Accessing from the sky: A tutorial on UAV communications for 5G and beyond," *Proc. IEEE*, vol. 107, no. 12, pp. 2327–2375, Dec. 2019.

[17] H. Wu, F. Lyu, C. Zhou, J. Chen, L. Wang, and X. Shen, "Optimal UAV caching and trajectory in aerial-assisted vehicular networks: A learning-based approach," *IEEE J. Sel. Areas Commun.*, vol. 38, no. 12, pp. 2783–2797, Dec. 2020.

[18] Z. Wang, R. Liu, Q. Liu, J. S. Thompson, and M. Kadoch, "Energy-efficient data collection and device positioning in UAV-assisted IoT," *IEEE Internet Things J.*, vol. 7, no. 2, pp. 1122–1139, Feb. 2020.

[19] Y. Sun, D. Xu, D. W. K. Ng, L. Dai, and R. Schober, "Optimal 3D-trajectory design and resource allocation for solar-powered UAV communication systems," *IEEE Trans. Commun.*, vol. 67, no. 6, pp. 4281–4298, Jun. 2019.

[20] M. Mozaffari, W. Saad, M. Bennis, and M. Debbah, "Unmanned aerial vehicle with underlaid device-to-device communications: Performance and tradeoffs," *IEEE Trans. Wireless Commun.*, vol. 15, no. 6, pp. 3949–3963, Jun. 2016.

[21] J. Zhang, Y. Zeng, and R. Zhang, "UAV-enabled radio access network: Multi-mode communication and trajectory design," *IEEE Trans. Signal Process.*, vol. 66, no. 20, pp. 5269–5284, Oct. 2018.

[22] Q. Wu, Y. Zeng, and R. Zhang, "Joint trajectory and communication design for multi-UAV enabled wireless networks," *IEEE Trans. Wireless Commun.*, vol. 17, no. 3, pp. 2109–2121, Mar. 2018.

[23] Y. Cai, Z. Wei, R. Li, D. W. K. Ng, and J. Yuan, "Joint trajectory and resource allocation design for energy-efficient secure UAV communication systems," *IEEE Trans. Commun.*, vol. 68, no. 7, pp. 4536–4553, Jul. 2020.

[24] X. Li, W. Feng, Y. Chen, C.-X. Wang, and N. Ge, "Maritime coverage enhancement using UAVs coordinated with hybrid satellite-terrestrial networks," *IEEE Trans. Commun.*, vol. 68, no. 4, pp. 2355–2369, Apr. 2020.
[25] J. Wang, C. Jiang, Z. Wei, C. Pan, H. Zhang, and Y. Ren, "Joint UAV hovering altitude and power control for space-air-ground IoT networks," *IEEE Internet Things J.*, vol. 6, no. 2, pp. 1741–1753, Apr. 2019.
[26] Y. Wang *et al.*, "Joint resource allocation and UAV trajectory optimization for space–air–ground Internet of remote things networks," *IEEE Syst. J.*, early access, Sep. 10, 2020, doi: 10.1109/JSYST.2020.3019463.
[27] H. Huang, S. Guo, W. Liang, K. Wang, and A. Y. Zomaya, "Green data-collection from geo-distributed IoT networks through low-earth-orbit satellites," *IEEE Trans. Green Commun. Netw.*, vol. 3, no. 3, pp. 806–816, Sep. 2019.
[28] J. P. Choi and V. W. S. Chan, "Predicting and adapting satellite channels with weather-induced impairments," *IEEE Trans. Aerosp. Electron. Syst.*, vol. 38, no. 3, pp. 779–790, Jul. 2002.
[29] M. J. Neely, E. Modiano, and C. E. Rohrs, "Dynamic power allocation and routing for time-varying wireless networks," *IEEE J. Sel. Areas Commun.*, vol. 23, no. 1, pp. 89–103, Jan. 2005.
[30] Q. Wu and R. Zhang, "Common throughput maximization in UAV-enabled OFDMA systems with delay consideration," *IEEE Trans. Commun.*, vol. 66, no. 12, pp. 6614–6627, Dec. 2018.
[31] Y. Zeng, R. Zhang, and T. J. Lim, "Throughput maximization for UAV-enabled mobile relaying systems," *IEEE Trans. Commun.*, vol. 64, no. 12, pp. 4983–4996, Dec. 2016.
[32] J. Zhang *et al.*, "Computation-efficient offloading and trajectory scheduling for multi-UAV assisted mobile edge computing," *IEEE Trans. Veh. Technol.*, vol. 69, no. 2, pp. 2114–2125, Feb. 2020.
[33] B. Qian, H. Zhou, F. Lyu, J. Li, T. Ma, and F. Hou, "Toward collision-free and efficient coordination for automated vehicles at unsignalized intersection," *IEEE Internet Things J.*, vol. 6, no. 6, pp. 10408–10420, Dec. 2019.
[34] D. P. Bertsekas, *Nonlinear Programming*. Belmont, MA, USA: Athena Scientific, 1999.
[35] M. Grant and S. Boyd. (Mar. 2014). *CVX: MATLAB Software for Disciplined Convex Programming, Version 2.1*. [Online]. Available: http://cvxr.com/cvx
[36] M. Hast, K. J. Astrom, B. Bernhardsson, and S. Boyd, "PID design by convex-concave optimization," in *Proc. Control Conf.*, 2013, pp. 4460–4465.
[37] T. Ma, H. Zhou, B. Qian, and A. Fu, "A large-scale clustering and 3D trajectory optimization approach for UAV swarms," *Sci. China Inf. Sci.*, vol. 64, no. 4, pp. 1–16, 2021.
[38] J. Magnus and H. Neudecker, *Matrix Differential Calculus With Applications in Statistics and Econometrics*, 3rd ed. New York, NY, USA: Wiley, 1986.
[39] D. P. Palomar and M. Chiang, "A tutorial on decomposition methods for network utility maximization," *IEEE J. Sel. Areas Commun.*, vol. 24, no. 8, pp. 1439–1451, Aug. 2006.
[40] D. Bertsekas, N. Angelia, and E. O. Asuman, *Convex Analysis and Optimization*. Belmont, MA, USA: Athena Scientific, 2003.

Ting Ma (Member, IEEE) received the B.S., M.S., and Ph.D. degrees in statistics from Sichuan University, Chengdu, China, in 2013, 2016, and 2020, respectively. She is currently a Post-Doctoral Fellow with the School of Electronic Science and Engineering, Nanjing University, Nanjing, China. Her main current research interests include robust hypothesis testing, space-air-ground integrated networks, convex optimization theory, and game theory.

Haibo Zhou (Senior Member, IEEE) received the Ph.D. degree in information and communication engineering from Shanghai Jiao Tong University, Shanghai, China, in 2014. From 2014 to 2017, he was a Post-Doctoral Fellow with the Broadband Communications Research Group, Department of Electrical and Computer Engineering, University of Waterloo. He is currently an Associate Professor with the School of Electronic Science and Engineering, Nanjing University, Nanjing, China. His research interests include resource management and protocol design in vehicular ad hoc networks, 5G/B5G wireless networks, and space-air-ground integrated networks. He won the 2020 Norbert Wiener Review Award of IEEE/CAA JOURNAL OF AUTOMATICA SINICA. He was named as the 2020 highly cited researcher in cross-field. He was a recipient of the 2019 IEEE ComSoc Asia–Pacific Outstanding Young Researcher Award. He has served as the Invited Track Co-Chair for ICCC 2019 and VTC-Fall 2020 and a TPC Member for many IEEE conferences, including GLOBECOM, ICC, and VTC. He has served as an Associate Editor for the IEEE Comsoc Technically Co-Sponsored the *Journal of Communications and Information Networks* (JCIN) from April 2017 to March 2019, and a Guest Editor for the IEEE TRANSACTIONS ON VEHICULAR TECHNOLOGY in 2021, the IEEE INTERNET OF THINGS JOURNAL in 2021, *IEEE Communications Magazine* in 2016, the *International Journal of Distributed Sensor Networks* (Hindawi) in 2017, and *IET Communications* in 2017. He is currently an Associate Editor of the IEEE INTERNET OF THINGS JOURNAL, *IEEE Network Magazine*, the IEEE WIRELESS COMMUNICATIONS LETTERS, and *JCIN*.

Bo Qian (Student Member, IEEE) received the B.S. and M.S. degrees in statistics from Sichuan University, Chengdu, China, in 2015 and 2018, respectively. He is currently pursuing the Ph.D. degree with the School of Electronic Science and Engineering, Nanjing University, China. His current research interests include intelligent transportation systems and vehicular networks, wireless resource management, blockchain, convex optimization theory, and game theory. He was a recipient of the IEEE VTC-Fall Best Paper Award in 2020.

Nan Cheng (Member, IEEE) received the B.E. and M.S. degrees from the Department of Electronics and Information Engineering, Tongji University, Shanghai, China, in 2009 and 2012, respectively, and the Ph.D. degree from the Department of Electrical and Computer Engineering, University of Waterloo, in 2016. He has worked as a Post-Doctoral Fellow with the Department of Electrical and Computer Engineering, University of Toronto, from 2017 to 2019. He is currently a Professor with the State Key Laboratory of ISN and the School of Telecommunication Engineering, Xidian University, Shaanxi, China. His current research interests include B5G/6G, space-air-ground integrated networks, big data in vehicular networks, and self-driving systems. His research interests also include performance analysis, MAC, opportunistic communication, and application of AI for vehicular networks.

Xuemin (Sherman) Shen (Fellow, IEEE) received the Ph.D. degree in electrical engineering from Rutgers University, New Brunswick, NJ, USA, in 1990.

He is currently a University Professor with the Department of Electrical and Computer Engineering, University of Waterloo, Waterloo, ON, Canada. His current research interests include network resource management, wireless network security, the Internet of Things, 5G and beyond, and vehicular ad-hoc and sensor networks.

Dr. Shen is a registered Professional Engineer in the State of Ontario, Canada, a fellow of the Engineering Institute of Canada, the Canadian Academy of Engineering, and the Royal Society of Canada, a Chinese Academy of Engineering Foreign Member, and a Distinguished Lecturer of the IEEE Vehicular Technology Society and Communications Society. He was a recipient of the Joseph LoCicero Award in 2015 and the Education Award in 2017 from the IEEE Communications Society, the James Evans Avant Garde Award from the IEEE Vehicular Technology Society in 2018, the R. A. Fessenden Award in 2019 from IEEE, Canada, the Award of Merit from the Federation of Chinese Canadian Professionals (ON) in 2019, and the Technical Recognition Award from the Wireless Communications Technical Committee in 2019 and AHSN Technical Committee in 2013. He was also a recipient of the Premiers Research Excellence Award from the Province of Ontario, Canada, in 2003, and the Excellent Graduate Supervision Award from the University of Waterloo in 2006. He was the Technical Program Committee Chair/Co-Chair of IEEE Global Telecommunications Conference in 2007, IEEE Vehicular Technology Conference in 2010, IEEE International Conference on Computer Communications in 2014, and IEEE Global Communications Conference in 2016, and the Chair for the IEEE Communications Society Technical Committee on Wireless Communications. He is the elected IEEE Communications Society Vice-President for Technical and Educational Activities, the Vice-President for Publications, Member-at-Large on the Board of Governors, the Chair of the Distinguished Lecturer Selection Committee, and a member of IEEE ComSoc Fellow Selection Committee. He was/is the Editor-in-Chief of the IEEE INTERNET OF THINGS JOURNAL, IEEE NETWORK, *IET Communications*, and *Peer-to-Peer Networking and Applications*.

Xiang Chen received the B.E. degree in electronics and information engineering from the Huazhong University of Science and Technology (HUST) in 2008 and the Ph.D. degree from the Department of Electronic and Computer Engineering, Hong Kong University of Science and Technology (HKUST), in 2013. After graduation, he was a Senior Engineer with the Hong Kong Applied Science and Technology Research Institute (ASTRI) from 2013 to 2019. He is currently with the Theory Laboratory, Huawei Hong Kong Research Institute, as a Principal Engineer. His broad research interests include system and algorithm design for emerging wireless technologies and theory, including massive MIMO, interfering networks, and B5G/6G cell-free architecture.

Bo Bai (Senior Member, IEEE) received the B.S. degree (Hons.) in communication engineering from Xidian University, Xi'an, China, in 2004, and the Ph.D. degree in electronic engineering from Tsinghua University, Beijing, China, in 2010.

From 2009 to 2012, he was a Research Assistant (from April 2009 to September 2010) and a Research Associate (from October 2010 to April 2012) with the Department of Electronic and Computer Engineering, The Hong Kong University of Science and Technology (HKUST). From July 2012 to January 2017, he was an Assistant Professor with the Department of Electronic Engineering, Tsinghua University. He has also obtained the support from the Backbone Talents Supporting Project of Tsinghua University. He is currently a Senior Researcher with the Future Network Theory Laboratory, 2012 Laboratories, Huawei Technologies Company Ltd., Hong Kong. He has authored more than 70 articles in major IEEE journals and flagship conferences, two book chapters, and one textbook. His research interests include hot topics in wireless networking, network information theory, network control, fog/edge computing, and massive network analysis. He has also served on the Wireless Communications Technical Committee (WTC) and the Signal Processing and Communications Electronics (SPCE) Technical Committee. He has served as a TPC Member for several IEEE ComSoc conferences, such as ICC, GLOBECOM, WCNC, VTC, ICCC, and ICCVE. He received the Honor of Outstanding Graduates of Shaanxi Province and the Honor of Young Academic Talent of Electronic Engineering, Tsinghua University. He was a recipient of the Student Travel Grant at IEEE GLOBECOM 2009. He was invited as a Young Scientist Speaker at IEEE TTM 2011. He was a recipient of the Best Paper Award in IEEE ICC 2016. He has also served as a reviewer for a number of major IEEE journals and conferences.